Mirjam Vera Pennauer, BSc

A pharmaco chemical approach to ribosome biogenesis

MASTER'S THESIS

to achieve the university degree of

Master of Science

Master's degree programme: Molecular Microbiology

submitted to

Graz University of Technology

Supervisor

Ao.Univ.-Prof. Mag. Dr.rer.nat. Helmut Bergler

Institute of Molecular Biosciences
University of Graz

Graz, March 2016

AFFIDAVIT

I declare that I have authored this thesis independently, that I have not used other than the declared sources/resources, and that I have explicitly indicated all material which has been quoted either literally or by content from the sources used. The text document uploaded to TUGRAZonline is identical to the present master's thesis.

Date

Signature

Danksagung

Danke an

Helmut
Gertrude
Brigitte
Dominik

für alles, was ich von euch lernen durfte, all die Gespräche und Scherze, all die Aufmunterungen und die tolle Zeit mit euch!

Danke an

alle weiteren Mitglieder der Bergler/Pertschy Arbeitsgruppe

ohne euch wäre die Zeit im Labor und diverse Feierlichkeiten nicht annähernd so lustig und unterhaltsam gewesen!

Danke an

David
Chrissi
Manfred
meine Schwester
meine Eltern

für die Unterstützung während der gesamten Zeit!

Abstract

During ribosome biogenesis in the yeast *Saccharomyces cerevisiae* rRNAs and ribosomal proteins are assembled into a large 60S and a small 40S subunit to form a mature ribosome. For this highly complex and very fast process a number of different small nucleolar RNAs and over 200 different assembly factors are required. The starting point of the biosynthesis is the transcription of a long pre-rRNA in the nucleolus and subsequent recruitment of assembly factors, forming a precursor particle, which then separates into a pre-40S and a pre-60S particle. On their way from the nucleolus through the nucleoplasm and subsequent export to the cytoplasm, maturation of these pre-ribosomal particles occurs, which includes binding and release of assembly factors, rRNA processing and remodeling.

Although the last decades of research have created a profound knowledge of ribosome biogenesis, many molecular details are still poorly understood. The perturbation or inhibition of the process at certain maturation steps using small-molecule substances might allow identification of currently undiscovered factors and help to provide a more detailed understanding. Besides the application in basic research, such inhibitors also harbor significant therapeutic potential regarding the treatment of hyperproliferative disorders like cancer.

Previous work in our laboratory led to the identification of more than one hundred potential inhibitors of ribosome biogenesis. The aim of this study was to investigate and further characterise selected examples of these potential inhibitors. Basic information should be obtained by investigation of the inhibitory potential by determining the minimal inhibitory concentration (MIC) and by estimating the kinetics of inhibition using fluorescence microscopy. In addition, a methodology should be developed to identify the target of the most promising potential inhibitor. The experimental approach combined the direct identification via screening of a mutant gene library and by monitoring the consequences of drug treatment on early pre-60S particles using tandem affinity purification (TAP) purifications. Taken together this study shows a strategy for the characterisation of potential inhibitors and an experimental approach for the identification of the target.

Zusammenfassung

Bei der Ribosomenbiogenese in *Saccharomyces cerevisiae* werden rRNAs und ribosomale Proteine zu einer großen 60S und einer kleinen 40S Untereinheit assembliert, welche ein reifes Ribosom bilden. Für diesen sehr komplexen und schnellen Prozess werden verschiedene kleine nukleare RNAs und über 200 unterschiedliche Assemblierungsfaktoren benötigt. Der Ausgangspunkt der Biogenese ist die Transkription einer langen Vorläufer-rRNA im Nukleolus und das darauf folgende Binden der Assemblierungsfaktoren. Dies führt zur Bildung eines Vorläuferpartikels, welcher sich dann in eine pre-40S und eine pre-60S Partikel aufspaltet. Auf dem Weg vom Nukleolus durch das Nukleoplasma und dem anschließenden Export ins Zytoplasma reifen die Partikel, wobei Assemblierungsfaktoren binden und abgelöst, die rRNA prozessiert und die Partikel umgeformt werden.
Obwohl durch die jahrzehntelange Forschung ein fundiertes Wissen der Ribosomenbiogenese geschaffen wurde, sind viele molekulare Details noch unzureichend verstanden. Diesbezüglich könnte die Störung oder Inhibierung eines bestimmten Reifungsschrittes in der Ribosomenbiogenese durch kleinmolekulare Substanzen zur Entdeckung von derzeit unbekannten Faktoren führen und helfen ein detaillierteres Wissen zu schaffen. Neben der Anwendung in der Grundlagenforschung haben solche Inhibitoren auch therapeutisches Potential bezüglich der Behandlung von hyperproliferativen Erkrankungen wie beispielsweise Krebs.

Frühere Arbeiten in unserem Labor führten zur Identifizierung von mehr als einhundert potentiellen Inhibitoren der Ribosomenbiogenese. Das Ziel dieser Studie war die Untersuchung und die weitere Charakterisierung von ausgewählten potentiellen Inhibitoren. Die grundlegenden Informationen sollen durch die Untersuchung des inhibitorischen Potentials durch Bestimmung der minimalen Hemmkonzentration (MHK) und durch die Abschätzung der Kinetik der Inhibierung durch Fluoreszenzmikrokopie erhalten werden. Zusätzlich soll eine Methode entwickelt werden, welche die Identifizierung des Angriffsorts des vielversprechensten potentiellen Inhibitors ermöglicht. Die experimentelle Herangehensweise besteht aus einer direkten Identifikation durch das Screening einer Mutanten-Genbank und durch die Untersuchung der Auswirkungen der Behandlung auf die frühen 60S Partikeln durch TAP Reinigungen. Zusammengefasst zeigt diese Studie eine Strategie für die Charakterisierung von potentiellen Inhibitoren, sowie eine experimentelle Herangehensweise für die Identifizierung des Angriffspunktes.

Table of content

1. Introduction

1.1. A short introduction to ribosome biogenesis in *Saccharomyces cerevisiae*

The ribosome is often referred to as a nanomachine, which translates the genetic code to proteins and thus is essential for any living cell. The ribonucleoprotein consists of two subunits, whereas the small 40S subunit comprises one rRNA (18S) and 33 different ribosomal proteins, while the large 60S subunit contains 3 rRNAs (5S, 5.8S and 25S) and 46 ribosomal proteins (Woolford and Baserga, 2013). Although ribosomes are highly complex structures, in a fast growing yeast cell more than 2000 ribosomes are assembled each minute (Warner, 1999). This enormous number gives an idea of how much energy and resources a cell spends on the synthesis of ribosomes. For instance, 60% of the total cellular RNA transcription is used for ribosome biogenesis and all three RNA polymerases are involved in this process. Already Kief and Warner (1981) showed that the ribosome content is proportional to growth rate.

Today we know, that for the assembly of the approximately 5500 nt of rRNA and the 79 ribosomal proteins into a ribosome, 76 different small nucleolar RNAs and over 200 different assembly factors are required. Since the 1970s, when researchers have begun to investigate the assembly of ribosomes, new methods like tandem affinity purification, mass spectometric methods and cryoelectron microscopy reconstructions have revealed many details of the ribosome biogenesis. But still many details are unknown (Woolford and Baserga, 2013). In short, the biogenesis of the ribosome starts in a subcompartement of the nucleus termed nucleolus. The nucleolus is formed around the approximately 150 tandem repeats of the rDNA, where the rDNA is transcribed (reviewed by Thiry and Lafontaine, 2005). Initially, the RNA polymerase I transcribes the 35S precursor rRNA, whereof after processing certain sections become part of the small or the large subunit, while others like the the external spacer (ETS) and the internal spacer (ITS) are processed away. The 5S rRNA is transcribed by the RNA polymerase III in the opposite direction. By assembly of the first ribosomal proteins and assembly factors to the 35S precursor rRNA the 90S particle is formed (figure 1). After the first rRNA processing step, this 90S particle separates into the pre-40S and pre-60S subunit. These precursor subunits contain many, but not all of the ribosomal proteins and assembly factors. Then the particles migrate from the nucleolus through the nucleoplasm, before they are exported to the cytoplasm. On their way, the precursor subunits mature and undergo remodelling, which includes for instance endonucleolytic and exonuclolytic processing of the rRNA, release and docking of assembly factors or modification by small nucleolar ribonucleoproteins (snoRNPs). Sometimes one of

these processing steps enables the next in a hierarchical manner and sometimes blocking an earlier step does not prevent a following step from occurring (reviewed Woolford and Baserga, 2013).

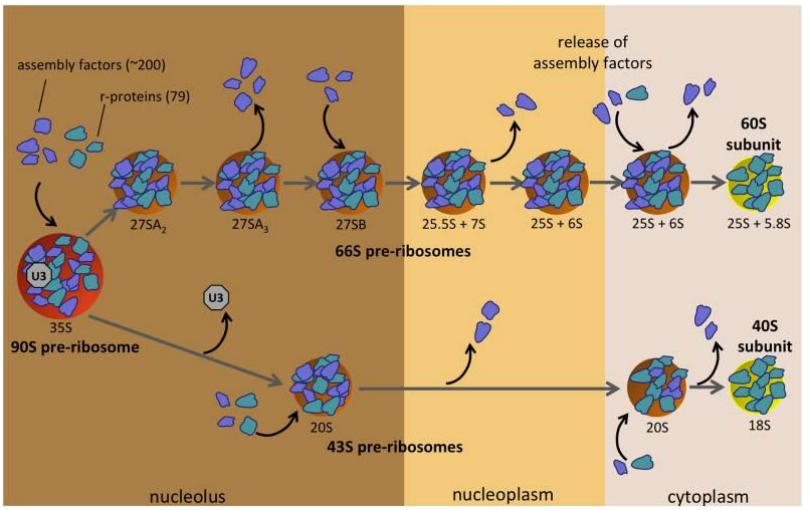

Figure 1: Overview of the maturation of the 60S and 40S subunits in *Saccharomyces cerevisiae*. Most of the ribosomal proteins (light blue) and many assembly factors (dark blue) bind to the precursor particle in an early phase. During the migration from the nucleolus through the nucleoplasm and the subsequent export to the cytoplasm, the precursor particle matures. This includes for instance rRNA processing and binding and release of assembly factors (taken from Woolford and Baserga, 2013).

1.2. Inhibitors of ribosome biogenesis and their relevance

The last decades of investigating the ribosome biogenesis have created a profound knowledge of the process, but still many molecular details remain unclear. One possible reason might be the deficiency in compounds for perturbation of the ribosome biogenesis. These inhibitors may allow revelation of currently undiscovered factors and help to provide a more detailed understanding. The small-molecule substances are thought to act like genetic mutations affecting the ribosome biogenesis. They might disable or slow down the assembly of the ribosome and thereby making it possible to isolate and study the immature subunits. This approach has particular advantages compared to genetic perturbations. For instance, the chemicals can exert their effects in a time scale of seconds and they can be added or removed as required. Moreover, particles that are studied in a genetically modified background may be thermodynamically stable off-pathway products. Nevertheless, one have to pay attention to dissect tightly linked processes or in other word, to avoid or recognise pleiotropy. Regarding this the target specify of inhibitors is a main point to allow meaningful conclusions (Stokes and Brown, 2015). The up to now only known example for a ribosome biogenesis inhibitor is diazaborine, which was shown to specifically block the maturation of the 60S ribosomal subunit in yeast (Pertschy et al., 2004). Later the AAA-

ATPase Drg1 was identified as the target of diazaborine. This protein releases the shuttling protein Rlp24 from pre-60S particles after their export from the nucleus. Binding of diazaborine to Drg1 prevents the ATP hydrolysis in D2 and thus the release of Rlp24 is blocked, which consequently halts downstream maturation of the pre-ribosome, (Loibl et al., 2014).

So far, the use of inhibitors for the basic research was emphasised, nevertheless the therapeutic potential has to be taken into account. Especially, the treatment of diverse hyperproliferative disorders like cancer has to be considered as ribosome biogenesis is tightly linked to growth (Stokes and Brown, 2015). In this context, the study of Burger et al. (2010) showed that many chemotherapeutic drugs, which are used for treatment of neoplastic diseases for more than 50 years, affect different aspects of rRNA synthesis. For many of these compounds, the actual targets are not well defined and results obtained in yeast may contribute to the identification of the mammalian target as many factors involved are conserved.

Another aspect is the connection between the ribosome biogenesis and the tumor suppressor p53. A real break-through was the study of Rubbi and Milner (2003). Therein they showed that p53 accumulates only upon UV irradiation if the nucleolus is affected. The damaging of the nuclear DNA alone failed to stabilise p53. Hence it was suggested that the nucleolus is a stress sensor responsible for maintenance of low levels of p53. Subsequently, it has been shown that several ribosomal proteins can bind and inactivate Mdm2, which is the ubiquitin ligase targeting p53 to the proteasome for degradation. Furthermore, inhibition of the ribosome biogenesis at the level of rRNA transcription or rRNA maturation consistently leads to an inactivation of Mdm2 and the stabilisation of p53. Thus a functional ribosome biogenesis is an essential prerequisite for inactivation of p53 in proliferating cells (Burger et al., 2010).

Also other findings clarify the link between cancer and ribosome biogenesis, like the abnormal nucleolar morphology in almost all cancer types is caused by the hyperactivation of rDNA transcription. Or that the transcription factor MYC, which is one of the most frequent activated oncoproteins, was identified as a master regulator of ribosome biogenesis (Quin et al., 2014).

1.3. The beginning of the project and the aim of this study

The overall aim of this project was to identify novel inhibitors of the ribosome biogenesis due to the new possibilities that would open up as mentioned in the previous paragraph.

The starting point of the project was the development of a screen for such inhibitors. The screen is based on the knowledge that most of the steps of the ribosome biogenesis occur in the nucleolus and nucleus and on the observation, that inhibition of maturation results in the accumulation of ribosomal reporter proteins in the nucleolus and/or the nucleoplasm (Hurt et al, 1999). Subsequently, over 1000 compounds from natural and medical compound libraries were screened (Dominik Awad, master thesis) for an accumulation of a ribosomal GFP fusion reporter protein. 130 potential inhibitors were identified.

Based on the data of this screen and on the observed changes of total rRNA composition upon treatment (Matthias Loibl, unpublished data) seven potential inhibitors were selected. The aim of this study was the further characterisation of these compounds. Basic information should be obtained by the determination of the minimal inhibitory concentration (MIC) and by measuring the kinetics of accumulation of the reporter protein by fluorescence microscopy. Thereupon, the target of the most promising potential inhibitor should be identified using UV mutagenesis for generation of a resistant mutant and construction of a gene library. For this purpose, an experimental approach should be developed. Additionally, a TAP purification should provide further information.

2. Material and Methods

2.1. Strains, plasmids, primers and antibodies

Strain	Genotype	Source	IMB No.	Info
W303a	Mat a; leu2; ura3; his3; ade2; trp1	Michael Durchschlag	1077	wildtype strain
C303a	Mat a; leu2; ura3; his3; trp1	Igor Podolsky	6580C	wildtype strain
C303a Rpl7a-GFP	C303a; C303a Rpl7a-GFP::HISMX	Domonik Awad	6598A	microscopy
C303a Δyap1	Mat a; leu2; ura3; his3; trp1; ypa1::HIS3;	This study		original strain for the gene library
Noc2-TAP	Mat a; his3; leu2; ura3; lys2; YOR206w-TAP (URA2-KL)	Uni Regensburg	6584B	TAP purification
E. coli XL-1	endA1, usdR17(rK-, mK+), supE44, thi-1, lamda-, recA1, gyrA96, relA1, delta (lac), F`, proAB, lac laZ delta M15, Tn10(Tet R)	Ira Fortuin	3771	electrocompetent *E. coli*
E. coli XL-1 pRS316	endA1, usdR17(rK-, mK+), supE44, thi-1, lamda-, recA1, gyrA96, relA1, delta (lac), F`, proAB, lac laZ delta M15, Tn10(Tet R) [pRS316]	DNA R. Leber; Transformation H. Grillitsch	3275	isolation of the vector pRS316

Plasmid	Info
3633_pFA6a His3MX	Template for knock out cassette
pRS316	Vector for the gene library

Primer	Primer sequence	Info
Yap1_fwd_S1	TTTTGCCACCCAAAACGTTTAAAGAAGGAAAAG TTGTTTCTTAAACCATGcgtacgctgcaggtcgac	Knockout *YAP1*
Yap1_rev_S2	ATAGAAAAAGTTCTTTCGGTTACCCAGTTTTCCA TAAAGTTCCCGCTTTAatcgatgaattcgagctcg	Knockout *YAP1*
Yap1_ko_ctrl	CGTCTTTGTCATGGGAACCGG	Colony PCR: knockout *YAP1*
KanMX5'	CAAGACTGTCAAGGAGGG	Colony PCR: knockout *YAP1*
Drg1seq1	ATGGCTCCTAAATCTAGT	Control PCR: gene library
Drg1seq2340	TTACGAAGATGAACCGCT	Control PCR: gene library
Nup116_fwd121	GGCCTCAGTCAGCAAACA	Control PCR: gene library
Nup116_rev2339	AAACTGGCTTTTTTGCGT	Control PCR: gene library
Nup159_1673f	CTTCCTTTGGCTCTGGAA	Control PCR: gene library
Nup159_rev3880	CTTTTTCCTTCAGGTCTT	Control PCR: gene library

Antibody	Source	Dilution	Host
Cbp	Sigma	1:5000	rabbit
Noc1	Uni Regensburg	1:5000	rabbit
Noc3	Uni Regensburg	1:5000	rabbit
Nog1	M. Fromont-Racine	1:5000	rabbit
Rpa135	M. Oaks	1:2000	rabbit

Rpl5	Woolford laboratory	1:30000	rabbit
Rpl16	S. Rospert	1:30000	rabbit
Rrp12	M. Dosil	1:5000	rabbit
α anti rabbit IgG	Sigma	1:15000	goat

2.2. Inhibitors and other chemicals

Inhibitor	Company (Product No.)	Solvent (concentration)
Acivicin	Sigma Aldrich (SML0312)	DMSO (10 mg/ml)
Carmofur	Sigma Aldrich (C1494)	DMSO (10 mg/ml)
Epirubicin hydrochloride	Sigma Aldrich (E9406)	DMSO (10 mM)
Mycophenolic Acid	Sigma Aldrich (M5255)	DMSO (10 mg/ml)
(+)-Usnic acid	Sigma Aldrich (329967)	DMSO (1 mg/ml)
Vulpinic acid	Santa Cruz Biotechnologie (CAS 521-52-8)	DMSO (10 mg/ml)

Chemicals	Company (Product No.)	Solvent (concentration)
Ampicillin	Carl Roth (K029.2)	water (100 mg/ml)
Cycloheximide	Sigma Aldrich (C7698)	ethanol (10 µg/µl)
4-Nitroquinoline N-oxide	Sigma Aldrich (N8141)	acetone (10 µg/µl)

2.3. Media and growth conditions

The media used for cultivation of *Saccharomyces cerevisiae* (*S. cerevisiae*) were the complete medium YPD and the minimal medium SD (see table 1), depending on the application. The pH of both media was adjusted to 5.5 and the medium was sterilised for 20 min at 125°C. Concerning the SD medium, two additional things had to be considered: The solution A and B had to be sterilised separately and the medium was supplemented with amino acids (see table 2). The SD medium containing all amino acids will be described as SD+all, whereas SD without, for instance, uracil will be denoted as SD-ura. Unless otherwise stated, the standard growing conditions were 30°C and if shaken using 170 rpm.

Table 1: Culture media for *S. cerevisiae*

Medium		Component	Concentration (g/l)
YPD		Yeast extract	10
		Pepton	20
		Glucose	20
		Agar (optional)	15-20
SD	Solution A	Yeast nitrogen base	1.4
		Ammonium sulfate	5
	Solution B	Glucose	20
		Agar (optional)	20
	Amino acid mix		1x

Table 2: Amino acid mix for supplementation of SD medium

Amino acid	Concentration 10x (g/l)	Final concentration 1x (mg/l)
Adenine sulfate	0.2	20
Uracil	0.2	20
L-Tryptophan	0.2	20
L-Histidine-HCl	0.2	20
L-Arginine-HCl	0.2	20
L-Methionine	0.2	20
L-Tyrosine	0.3	30
L-Leucine	0.3	30
L-Isoleucine	0.3	30
L-Lysine-HCl	0.3	30
L-Phenylalanine	0.5	50
L-Glutamic acid	1	100
L-Aspartic acid	1	100
L-Valine	1.5	150
L-Threonine	2	200
L-Serine	4	400

For the cultivation of *Escherichia coli* (*E. coli*), either 2xTY, LB or SOC medium was used (table 3), depending on the application. The media were sterilised for 20 min at 125°C. The standard growing conditions were 37°C and if shaken using 170 rpm.

Table 3: Culture media for *E. coli*

Medium	Component	Concentration (g/l)
2xTY	Trypton	16
	Yeast extract	10
	NaCl	5
	Agar (optional)	15
LB	Trypton	10
	Yeast extract	5
	NaCl	5
	Agar (optional)	15
SOC	Trypton	20
	Yeast extract	5
	Glucose	3.6
	NaCl	0.5
	KCl	0.186
	$MgSO_4$	4.8

2.3.1. Preparation of agar plates containing additives

The agar was prepared as described above. After the sterilisation, the agar was cooled down in a waterbath to 50°C before the compound was added and equally distributed by stirring with a magnetic mixer. In case that usnic acid had to be added, the stirring time was

prolonged to 4-5 min. The agar plates were precautionally dried in the dark at room temperature. Moreover, the plates were not stored, but fresh plates were prepared for each experiment.

2.4. Strain construction

2.4.1. Construction of the cassette for the knockout of *YAP1*

The cassette for the knockout of *YAP1* via homologous recombination was amplified via PCR using Yap1_fwd_S1 and Yap1_rev_S2 as primers and 3633_pFA6a His3MX as template. The detailed setup is shown in table 4 and 5.

Table 4: PCR reaction mix for amplification of the knockout cassette

Component	Volume (µl)
3633_pFA6a His3MX (~50 ng)	1
Taq Polymerase (NEB) (5 U/µl)	0.25
ThermoPol Buffer (NEB) (10x)	5
dNTPs (2 mM)	5
Yap1_fwd_S1 (20 µM)	1
Yap1_rev_S2 (20 µM)	1
Aqua bidest. (Fresenius)	36,75
Total	**50**

Table 5: PCR temperature profile for amplifying the knockout cassette

Step	Temperature °C	Time	Cycles
Initial Denaturation	95	30"	1
Denaturation	95	15"	
Annealing	55	30"	35
Amplification	72	1.5'	
Final elongation	72	5'	1
Hold	4	∞	

2.4.2. Preparation of amplified DNA for transformation

The amplified DNA was separated on an agarose gel (1%) and the appropriate band was cut out. Afterwards the DNA was cleaned up using the Gene Jet Gel Extraction Kit (Thermo Scientific) and eluted in 30 µl bidest. water (Fresenius). Then 1-2 µl were used for an agarose gel (1%) to determine the DNA concentration using the λ EcoRI HindIII standard (Thermo Scientific) for comparison. The remaining purified DNA was stored at -20°C.

2.4.3. Yeast transformation

The used standard protocol is based on Gietz (2014). The main culture (50 ml YPD) was inoculated to an OD_{600} of 0.2 (Beckman DU 640 Spectrophotometer) using an ONC. By the

time the culture reached an OD_{600} of 0.6-0.8, cells were harvested by centrifugation at 2200 rcf for 5 min at room temperature. Then, after two washing steps with lithium acetate (LiAc), the pellet was resuspended in 300 µl LiAc and the suspension was incubated at 30°C for 20 min. Meanwhile, the carrier DNA was prepared by denaturation for 10 min at 95°C and immediate cooled down on ice. For the transformation, all components (for details see table 6) were mixed, whereas additionally a negative (no DNA) and a positive control (known amount of plasmid DNA) were performed.

Table 6: Composition of the transformation mix

Component	Volume (µl)
Cells in LiAc	50
PCR product or plasmid	equal to 1-10 µg or 0.2-1 µg
Carrier DNA (10 mg/ml)	5
PEG	300

Then the cells got incubated at 30°C for 30 min, subsequently heat shocked at 42°C for 20 min. Immediately after this step, the cells were plated on an appropriate selective media or plated on non-selective media to be replicaplated on selective media the following day.

2.4.4. Colony PCR for verification of the correct integration

First, the transformants were striked out from the selective media plates on YPD plates. The next day, cell material equivalent to one colony was resuspended in 20 µl water (Fresenius) and incubated 10 min at 95°C for lysis. Then, the probes were cooled down on ice and afterwards centrifuged at 15700 rcf for 10 min. Meanwhile, the PCR mix has been prepared, to which the given amount of supernatant was added (see table 7). For the negative control the supernatant of the original strain was used. The temperature profile is shown in table 8. The result of the colony PCR was examined on an agarose gel (1%).

Table 7: Colony PCR mix

Component	Volume (µl)
Supernatant	7.5
Taq Polymerase (NEB) (5U/µl)	0.5
ThermoPol Buffer (NEB) (10x)	2.5
dNTPs (2mM)	2
Forward primer (20µM)	1
Reverse primer (20µM)	1
Aqua bidest. (Fresenius)	10,5
Total	**25**

Table 8: Colony PCR temperature profile

Step	Temperature °C	Time	Cycles
Initial Denaturation	95	5'	1
Denaturation	95	1'	
Annealing	55	1'	35
Amplification	72	2'	
Final elongation	72	5'	1
Hold	4	∞	

2.5. Agarose gel electrophoresis

Whenever DNA was examined using an agarose gel, the following procedure was used unless otherwise stated. The gel was made of 1x TAE puffer, 1% agarose and 0.2 µg/ml ethidium bromide (Sambrook et al., 1989). An appropriate amount of DNA was mixed with 6x loading dye (Thermo Scientific) and water (Fresenius) to a final concentration of 1x loading dye and a reasonable volume. For the migration of the DNA through the gel, 0.5x TAE served as a running buffer and the voltage was set to 7.5 V per centimeter gel length. The separated DNA fragments were detected and imaged in an UV cabinet with a camera. The size of the fragments was determined by comparison to a DNA standard (λ EcoRI HindIII, Gene ruler 100 bp or GeneRuler 1 kp, Thermo Scientific).

2.6. Fluorescence microscopy: Investigation of the kinetics of inhibition

Main cultures of the C303a and the C303a Rpl7a-GFP strain were inoculated in SD+all medium to an OD_{600} of 0.1 using an ONC and were grown to an OD_{600} of 0.4-0.6. Two aliquots of 500 µl were transferred into eprouvettes. For each strain one aliquot was treated with the potential inhibitor and to the other, which functioned as a control, the same amount of DMSO was added. After given treatment periods (0 min (=untreated), 15 min, 30 min, 60 min, 90 min and 120 min and if necessary also 180 min, 240 min, 300 min and 360 min) an aliquot was inspected by microscopy. From each image section, a DIC (differential interference contrast) and a fluorescence image were taken. A Zeiss Axioskop Fluorescence microscope with a magnification of 40x (objective) and secondary magnification of 1.6x was used. The fluorescence images were taken using a narrow band enhanced GFP (eGFP) filter from Zeiss and an exposure time of 1000 or 1500 ms.

2.7. UV mutagenesis

For the determination of the mortality curve, the main culture (SD+all medium) was inoculated to an OD_{600} of 0.1 using an ONC and grown to an OD_{600} of 0.4-0.6. Then the suspension was diluted to an OD_{600} of 0.1 and after a further diluting step (1:750), 100 µl

were plated on 10 SD+all plates each. For any tested UV dose (0, 2.5, 5, 7.5 or 10 mJ/cm^2) two plates were exposed. Evaluation was carried out after 2 or 3 days.
The calculated radiation dose was then used to irradiate cell using the same procedure and the conditions were chosen so that 20000 cells survived per plate. Five of these plates were replicaplated on SD+all+40µM usnic acid to screen for resistant mutants, which were then purified by striking them out again on solid selective media.

2.8. Spotting assay

The respective strains were grown over night in SD+all medium. The following day, aliquots were diluted to an OD_{600} of 0.3 with water (Fresenius). Afterwards, 220 µl of the suspension were transferred into a sterile 96 well plate and therein diluted three times 1:10 with water (Fresenius) to a total volume of 200 µl in each well. Then the cell suspensions were spotted on appropriate plates and incubated at various temperatures. At reasonable and regular intervals pictures were taken.

2.9. Determination of the minimal inhibitory concentration (MIC)

The selected strain was first grown as an ONC in SD+all medium, which was then used for inoculation of a main culture to a starting OD_{600} of 0.1. The cells were incubated until reaching an OD_{600} of 0.4-0.6. Then the suspension was diluted with medium to an OD_{600} of 0.05 and transferred into a 96 deep-well plate (200 µl per well), whereas the outermost wells were filled with 500 µl of water. This should minimise the evaporation and hence the loss of volume in the monitored wells. A certain amount of inhibitor or DMSO was added to the cells. Due to the diverging volume of added compound and thus DMSO, DMSO was added to each of the wells containing the potential inhibitor, until this difference was evened out. After covering the plate with a cell culture membrane, the cells were incubated at 28°C with 320 rpm. After 24 h the OD_{600} was measured in a 1:10 dilution and after 48 h in a 1:20 dilution.

2.10. Construction of a gene library

2.10.1. Isolation of genomic DNA

This protocol for genomic DNA isolation was based on Piper (1996) with the cell lysis procedure modified using a lab intern procedure.
The selected mutant was grown over night in YPD and 3 ml of the ONC were used to inoculate a 500 ml culture in YPD. After 16-24 h of growth, the cells were harvested by

centrifugation for 5 min at 1200 g at room temperature. The cell pellet was resuspended in 10 ml of sorbitol solution (0.9 M sorbitol, 0.1 M Tris-HCl pH 8.0, 0.1 M EDTA). To prepare the spheroblasts, 10 mg of zymolyase in 250 µl sorbitol solution and 20 µl of β-mercaptoethanol were added and the suspension was gently mixed by vortexing. Cells were spheroblasted under shaking (approximately 200 rpm) in a waterbath at 37°C for 1 h. The progress of cell wall digestion was monitored occasionally by mixing of a small aliquot of the cell suspension and distilled water on a microscope slide and subsequently microscoped. Spheroblasts were collected by centrifugation for 5 min at 1200 g at room temperature and washed twice with sorbitol solution (1.2 M sorbitol, 10 mM Tris-HCl pH 8.0). For the lysis of the spheroblasts, the pellet was resuspended in 10 ml of 100 mM Tris-HCl pH 8.0, 10 mM Na_2EDTA, 1% w/v SDS and 0.05 mg/ml proteinase K, which was added from a 10 mg/ml stock right before use. Protein digestion was carried out at 37°C for 60 min, followed by 65°C for 15 min and a final cool down to room temperature. An equal volume of 1:1 phenol:chloroform was added to the suspension and mixed by inversion. Phase separation was achieved by centrifugation at 4500 rcf for 10 min. The upper aqueous phase was transferred to a fresh tube and re-extracted with chloroform. Afterwards, the aqueous phase was transferred into a fresh vial and the DNA was precipitated with 2 vol ice cold ethanol and kept on ice for 30 min. The fibrous DNA was collected by spinning down with 1200 rcf for 5 min. After addition of 10 ml TE buffer, the DNA was dissolved over night and RNA was removed by RNase A addition to a final concentration of 50 mg/l and incubation at 37°C for 30 min. After an additional phenol:chloroform and a chloroform extraction, the DNA was precipitated by adding 0.04 vol 2 M NaOAc and 2 vol of ice cold ethanol. After 30 min on ice, the DNA was collected at 4500 rcf for 10 min. The DNA pellet was dried at room temperature and redissolved over night in 3 ml TE buffer. The DNA was stored at 4°C.

2.10.2. Partial digestion of genomic DNA with Bsp143I

The conditions for a convenient partial digestion had to be tested out each time, as the enzyme activity might vary due to residual ethanol from the purification. The amount of enzyme was kept fixed to 0.1 U Bsp143I/µg DNA, whereas the incubation time for digestion was varied. For the time series, a digestion mix was prepared and split into 10µl samples, which were incubated at 37°C for 5, 10, 15, 20, 25, 30 and 35 min. The enzyme was inactivated by addition of 0.5 µl 0.5 M EDTA pH 8 and subsequent incubation at 65°C for 20 min.

This procedure was used to identify the optimal digestion conditions for the later cloning of genomic DNA.

2.10.3. Fractionation of genomic DNA fragments

This protocol is based on the publication of Harnpicharnchai et al. (2007).

The partial digested DNA was loaded onto an agarose gel, next to a λ EcoRI HindIII standard (Thermo scientific) leaving one slot empty in between. A voltage of 85 V was applied for 35-45 min. Before proceeding, it was crucial that the DNA has migrated into the gel. Then, the power supply was switched of and the gel with the tray was put on an UV screen. By using the standard as a reference, a well of 3-4 mm width was cut into the gel in the lane of the DNA fragments right beneath the height of the smallest fragments to be collected. The UV exposure should be as short as possible, to minimise DNA damages. After that, the gel was put back into the running camber and the newly cut well was filled with PEG solution (30% PEG8000 in 1x TAE buffer). The voltage was applied again, so that the DNA migrated into the PEG solution. From then on, 10 times every 15 min the power was switched of and the PEG solution in the well was exchanged with new one. The PEG solution containing the DNA fragments was transferred into a tube and filled up to 2 ml with water (Fresenius). Each of the 10 gathered fractions was then split equally into four tubes. The DNA fragments were purified by extraction with an equal volume of 1:1 phenol:chloroform, phase separation by centrifugation at 4500 rcf for 10 min and a re-extraction of the aqueous phase with chloroform. Then, the DNA fragments in the aqueous phase were precipitated by addition of 0.04 vol 2 M NaOAc and 2 vol of ice cold ethanol. The tubes were kept on ice for 30 min. Then they were centrifuged at 4500 rcf for 10 min and the DNA pellets were dried and dissolved in 20 µl TE buffer over night. An aliquot of each fraction was loaded on an agarose gel for examination. The fraction with fragments between approximately 3 kb and 10 kb were pooled.

2.10.4. Preparation of the vector pRS316 for ligation

A sufficient amount of the vector pRS316 was cleaved with BamHI using 2.5 U/µg vector for 2 h at 37°C. After that, 1 U of alkaline phosphatase was added to each 20 µl sample, which contained approximately 1.5 µg plasmid DNA, for 20 min at 37°C. The mix was directly loaded onto a preparative agarose gel. The band of the cleaved vector was cut out of the gel, purified with the Gene Jet Gel Extraction Kit (Thermo Scientific) and eluted in 30 µl bidest. water (Fresenius).

2.10.5. Ligation of pRS316 with genomic DNA fragments

The ligation mix consisted of 250 ng cleaved and cleaned up vector, 1 U of T4 DNA ligase (Thermo Scientific), 2 µl ligase buffer and the genomic DNA fragments. As the fragments should be added in excess, the maximum amount was added, so that the volume of the mix did not exceed 20 µl. For the religation control, the DNA fragments were replaced by water. Ligation was performed for 2 h at room temperature.

2.10.6. Preparation of electrocompetent *E.coli* XL1 for transformation

The *E.coli* XL1 strain was grown in LB medium and 100 ml LB medium were incubated with 2 ml of the ONC. The main culture was incubated to an OD_{600} of 0.5-0.7 and then immediately placed on ice for 10 min. The cells were transferred into pre-cooled tubes and centrifuged for 7 min at 4500 rcf and 4°C. The supernatant was discarded and the pellet was carefully resuspended in 100 ml ice cold water in total. After another centrifugation step, the supernatant was discarded again and the pellet was resupended in 10 ml ice cold 10% glycerin in total. The suspensions were unified and centrifuged once more. The supernatant was removed entirely and the cell pellet was resuspended in 800 µl 10% glycerin. The cells were split in 50 µl aliquots, immediately frozen in liquid nitrogen and stored at -70°C.

2.10.7. Transformation of the ligated plasmids into electrocompetent *E. coli* XL1

First, the ligation mix was desalted for 1 h using MF membrane filters 0.025µm (Millipore), the electroporation cuvettes were sterilised by UV irradiation for 5 min and the *E. coli* XL1 cells were thawed on ice. The procedure was carried out for each aliquot as follows: 2 µl of the desalted ligation mix was added to the cells, which then got transferred into the cuvette and put into the electroporator (multiporator, Eppendorf). The used setting was 2500 V τ 5 ms. After the electroshock, 1 ml of SOC medium was added to the cells as quick as possible and the cells were regenerated at 37°C for 30 min. For generation of the gene library 16 aliquots of *E. coli* XL1 were used, as well as 2 aliquots of NEB 10 –beta electrocompetent *E. coli* cells (NEB). One additional aliquot was used for the religation control and one for the negative control. Each sample was plated out on five 2xTY plates containing ampicillin (100 µg/ml).

2.10.8. Isolation of the gene library plasmids

After one day of growth, the transformed *E. coli* were scraped off the plates using the smallest volume of LB medium possible. The suspension was incubated for 30 min. Then an aliquot of the cell suspension was used for isolation of the plasmids via PureYield™ Plasmid Midiprep System (Promega) following the vacuum protocol. The remaining cells were mixed 1:1 with 60% gylcerin and frozen at -70°C. The yield of the purification was determined using the nanodrop (NanoDrop ND 1000, Prelab, VWR International).

2.10.9. Controls for examination of the gene library

2.10.9.1. Screening for several genes via PCR

By performing a PCR with various primers (see section 2.1. Strains, plasmids, primers and antibodies), the gene library was screened for *DRG1*, *NUP116* and *NUP159*. For the composition of the PCR mix see table 9 and for the temperature profile table 10. The result of the PCR was examined via agarose gel electrophoresis.

Table 9: PCR reaction mix for verification of a gene

Component	Volume (µl)
Taq Polymerase (NEB) (5 U/µl)	0.5
ThermoPol Buffer (NEB) (10x)	2.5
dNTPs (2 mM)	2.5
Aqua bidest. (Fresenius)	13,5
Gene library plasmids or water (Fresenius)	5
Forward primer (20 µM)	0,5
Reverse (20 µM)	0,5
Total	**25**

Table 10: Temperature profile for the control PCR

Step	Temperature °C	Time	Cycles
Initial Denaturation	95	40"	1
Denaturation	95	20"	
Annealing	55	30"	35
Amplification	72	2.5'	
Final elongation	72	7'	1
Hold	4	∞	

2.10.9.2. Restriction analysis

By linearisation of the gene library plasmids, the size of the inserts should be estimated. For that purpose, 5µl gene library plasmids were digested with 1 U NotI for 1 h and the DNA fragments were separated on an agarose gel (1%).

2.10.9.3. Screening for selected genes via transformation

An aliquot of the gene library plasmids (4 µl) was transformed into a W303a strain as described earlier (section 2.4.3. Yeast transformation). One transformation mix was plated on SD-ura medium for determination of the transformation rate. For screening the transformants for the presence of the *HIS3* and the *ADE2* genes the cells were plated on SD-his and SD-ade medium.

2.11. TAP purification

2.11.1. TAP purification using magnetic beads for western and northern blots

The Noc2-TAP strain was grown in a 2 L culture (30°C, 110 rpm) of SD+all medium, which was inoculated using an ONC. At the time, the culture reached an OD_{600} of 1, the cells were treated with 80 µM usnic acid for 30 min. The adequate amount of DMSO was added to the untreated control for the same time.

The cells were harvested by centrifugation at 4°C for 5 min and 6200 rcf. The cell pellets were resuspended in 5-10 ml ddH_2O containing the same concentration of usnic acid or DMSO respectively. The suspensions were transferred into tubes and centrifuged with the setting indicated before. The supernatant was discarded and the pellets were directly processed or frozen at -70°C.

If cells were frozen, they were thawed on ice. The pellets were resuspended in 10 ml LB1 buffer (20 mM Hepes, 10 mM KCl, 2.5 mM $MgCl_2$, 1 mM EGTA, pH 7.5) supplemented with 1x FY (protease inhibitor mix, Serva, stock: 100x), 0.5 mM PMSF (phenylmethanesulfonyl fluorid, Sigma Aldrich, stock: 100 mM), 1 mM DTT (VWR, stock: 1000 mM), 0.02 U/µl RiboLock RNase inhibitor (LifeTech, stock: 40 U/µl) and 7.5 glass beads. Cells were disrupted in the disintegrator (Braun) for 4 min with CO_2 cooling. Whole cells and larger cell fragments were removed by centrifugation at 4°C for 10 min at 4500 rcf. The supernatant was transferred and centrifuged 10 min and after another transfer 30 min at 4°C with 41000 rcf. Meanwhile, the magnetic beads were prepared. For each sample, 150 µl beads (Bc Mag epoxy activated magnetic beads (Bioclone) coupled with rabbit IgG) were washed three times. At each washing step, 9 ml LB1 were added, the tube was put on a wheel for 3 min and the buffer was discarded using a magnet to separate the beads. Aliquots (30 µl) of the obtained crude extracts were frozen at -20°C for the protein gel and another 30 µl were stored at -80°C for the northern blot. The rest of the supernatant was transferred onto the beads and the tube was put on a wheel (10 rpm) for 90 min at 4°C for binding.

Hereafter, the unbound proteins were removed by washing two times with 9 ml LB1 and one time with LB1+100 mM NaCl. Then, the beads were suspended in 1ml of LB1+100 mM NaCl. At this point, one third of each sample was removed for the norther blot. After removing the supernatant, the beads were stored at -80°C. The remaining two thirds of each sample were prepared for the western blot. These aliquots were stepwise transferred into a 0.2 ml PCR tube and the supernatant was removed. Then, 50 µl of LB1+100 mM NaCl and 2 µl TEV protease were added to each sample to cleave off the protein A motive from the TAP tag. The tube was rotated on a wheel (10 rpm) at room temperature for 90 min for cleavage. The beads were removed by transferring the supernatant three times and afterwards, the samples were stored at -20°C.

2.11.2. SDS-polyacrylamide gel electrophoresis (SDS-PAGE)

First, the samples and the protein standards (unstained protein MW marker and PageRuler prestained protein ladder, both Thermo Scientific) had to be prepared by adding FSB (final sample buffer; stock 5x: 0.06 M Tris HCl, pH 6.8, 2% (w/v) SDS, 5% (v/v) β–mercaptoethanol, 8% (v/v) glycerin, 0.04% bromphenolblue;) to a final concentration of 2x. Then, the samples and the unstained protein standard were denaturated at 95°C for 10 min. The probes were loaded onto a 4-12% Bis-Tris gradient gel (Novex). For the separation, 1x NuPage MOPS buffer (Novex, stock: 20x) was used as running buffer and 100 V were applied for approximately 2 h. The proteins were then either detected by coomassie staining or blotted and detected using antibodies.

2.11.3. Coomassie staining

The separated proteins were stained using the Colloidal Blue Staining Kit (Novex) and following the manual´s instructions for staining NuPAGE Novex Bis-Tris gels. Alterations of the protocol were the reduction of the used volume to 11 ml, the staining over night and the washing step, as the gel was washed with water only until no background was seen and the gel was stored in 3% acetic acid.

2.11.4. Western blot

Once the proteins were separated by SDS-PAGE, they were blotted onto a PVDF membrane (Millipore) using a tank-blot-system (BioRad) with CAPS buffer (10 mM CAPS pH 11, 10% methanol). For the transfer, 220 mA were applied for 90 min. The nonspecific binding

sites were blocked by incubating the membrane in 1x TST (10x stock: 500 mM TRIS HCl, pH 7.4, 1.5 M NaCl, 1% Tween20) with 0.5% milk powder at 4°C over night.
The following day, the membrane was incubated with the primary antibody, which had been diluted in 1x TST with 0.5% milk powder. After 1 h of incubation at room temperature, the antibody solution was removed and the membrane was washed three times for 5 min with 1x TST. Then the secondary antibody, which was diluted in 1x TST with 0.5% milk powder, was added to the membrane and incubated for 1 h. Subsequently, the membrane was washed three times with 1xTST. The addition of a Western ECL substrate solution (BioRad) enables the detection of the proteins due to the chemiluminescence signal using the ChemiDocTouch imaging system (BioRad). Afterwards, the membrane was washed three times with 1x TST, before the stripping solution (10% SDS, 500 mM Tris-HCl, pH 6.7, 375 µl β-mercaptoethanol) was added and incubated for 20-30 min at 50°C to remove the bound antibodies. The membrane was washed four times for 5 min to remove any stripping solution left. For detection with a second antibody, nonspecific binding sites were blocked either with 1x TST with 3% milk powder for 30 min or with 1xTST and 0.5% milk powder over night and the process outlined above was repeated. For storage, the membrane was dried. All antibodies used, are listed in section 2.1. Strains, plasmids, primers and antibodies.

3. Results

3.1. Determination of the minimal inhibitory concentration (MIC)

The determination of the minimal inhibitory concentration (MIC) of the potential inhibitors should provide the basic information for the subsequent experiments. In general, the MIC is defined as "the lowest concentration of an antimicrobial that will inhibit the visible growth of a microorganism after overnight incubation" (Andrews, 2001). In my case, this definition was modified due to the determination of growth by the measurement of the OD_{600}. Thus, the MIC was redefined as the concentration of an inhibitor, which inhibited growth and an increase of the concentration did not lead to a significant lower OD_{600} after 24 h. Additionally, the growth after 48 h treatment was investigated to gather information for long-term applications, for instance the use as additive of agar plates. For each of the potential inhibitors, the impact on the growth of the C303a and the C303a Δyap1 strain was investigated (figure 2; summarised in table 11).

For acivicin, the MIC in the C303a strain was 40 µM, whereas after 48 h the same concentrations showed less growth inhibition compared to 24 h. In the C303 Δyap1 the MIC was 20 µM. After 48 h of incubation, the effect on the growth was lower than at 24 h at the resembling concentrations. Carmofur had its MIC also at 40 µM in the C303a strain and after 48 h the effects of the inhibitor on the growth were also reduced in comparison to 24 h treatment with the same concentrations. The MIC was with 20 µM lower in the C303 Δyap1 strain, whereas the inhibitory effect was again lower after 48 h incubation. The MIC of curcumin was between 40-80 µM in the C303a strain and lower in the C303 Δyap1 strain with 30 µM. In both strains no significant inhibition of growth was observed after 48 h. In the case of epirubicin, the MIC was around 250 µM in the C303a strain, whereas the same concentrations showed lower effect on the growth after 48 h of incubation. In the C303 Δyap1, the MIC was 150 µM, thus lower than in the C303a strain, whereas at 48 h the inhibitory effect was also reduced in comparison to the one at 24 h. In the case of mycophenolic acid, in both strains at 24 and 48 h, no significant inhibition of growth was observed by the concentrations tested. The concentration of 40 µM was determined as the MIC of usnic acid. After 48 h, the effect of the inhibitor was lower than at the same concentrations at 24 h. The MIC in the C303 Δyap1 strain was also 40 µM, whereas no examined concentration showed an inhibition of growth after 48 h. For vulpinic acid, no MIC was determined, since no concentration tested showed an inhibitory effect on the growth of either strain.

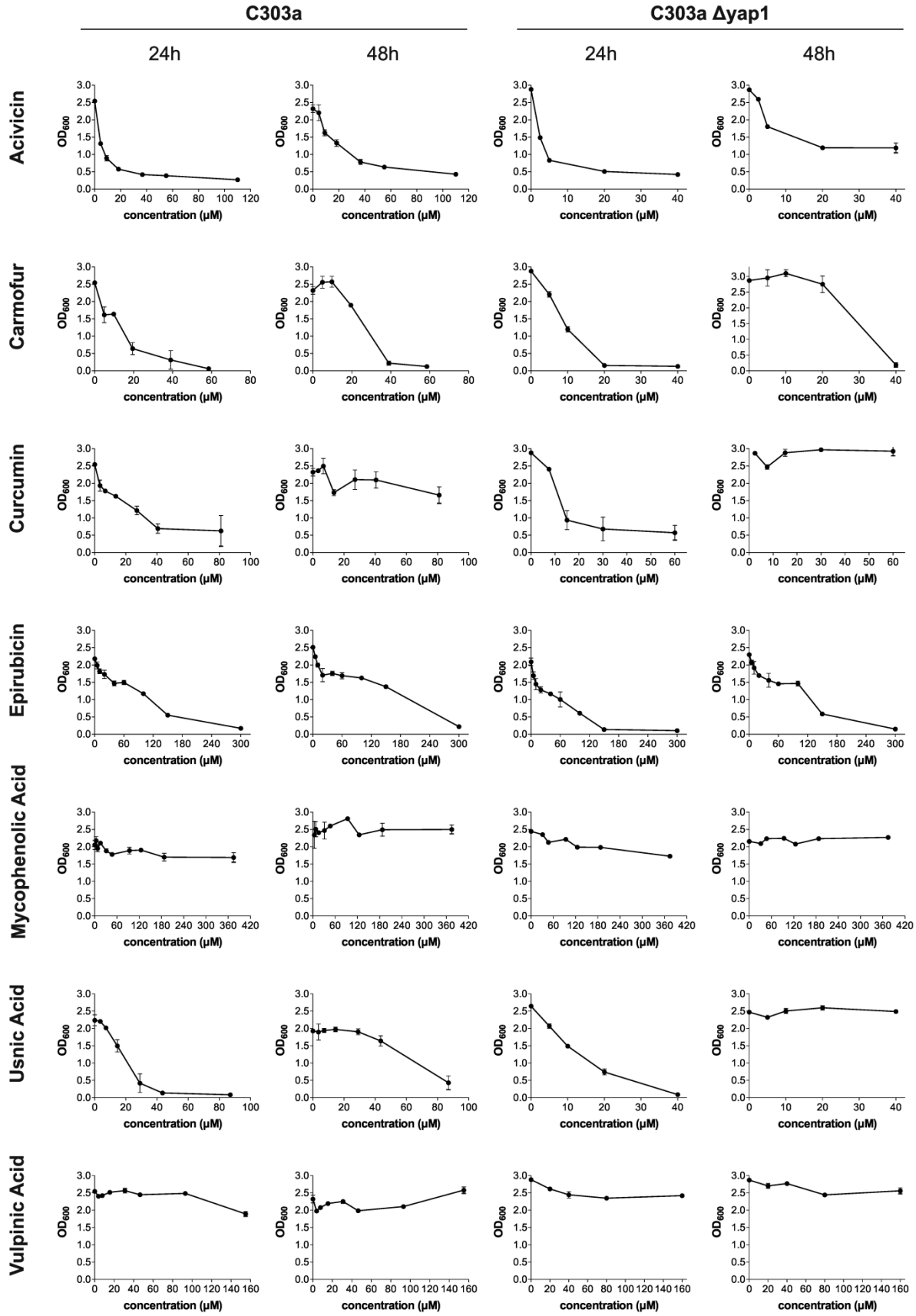

Figure 2: Determination of the MIC of potential inhibitors of the ribosome biogenesis by measurement of the OD_{600} after incubation in the presence of various drug concentrations. Each inhibitor was tested in the C303a and the C303 Δyap1 strain, whereas the OD_{600} was determined after 24 h and 48 h of incubation. The MIC was in this case defined as the concentration, which inhibited the growth of the cells and an increase of the concentration did not lead to a significant lower OD_{600} after 24 h. The behaviour after 48 h provides information for long-term applications.

Table 11: Overview of the MICs of the potential inhibitors

Potential Inhibitor	MIC	
	C303a	C303 Δyap1
Acivicin	40µM	20µM
Carmofur	40µM	20µM
Curcumin	40-80µM	30µM
Epirubicin	250µM	150µM
Mycophenolic acid	no inhibition	no inhibition
Usnic acid	40µM	40µM
Vulpinic acid	no inhibition	no inhibition

The MIC for most of the investigated inhibitors was determined and ranged between 20 to 250 µM, whereas the MIC in the C303 Δyap1 strain was, as expected, lower than in the C303a strain. Another general observation was that the same concentrations of a potential inhibitor showed lower effect on the growth after 48 h than after 24 h. Reasons might be that the compounds themselves are not stable or the cells can metabolise the potential inhibitors. Alternatively, the effectivity of the inhibitors might get influenced by a change in conditions caused by the cell growth, for instance a change in pH. Nonetheless, it is possible now to select the appropriate concentration of a compound for each application based on the obtained data.

3.2. Investigating the kinetics of the inhibition of ribosome biogenesis by fluorescence microscopy

Cells expressing the ribosomal GFP fusion protein Rpl7a-GFP were investigated by fluorescence microscopy after different times of incubation with the potential inhibitor. Primarily, the occurrence of an accumulation of the GFP signal in the nucleolus and/ or the nucleus was investigated. In untreated cells, the Rpl7a is in the steady state mainly localised in the cytoplasm, thus the GFP signal is visible in the cytoplasm, whereas no signal can be detected in the nucleus and the vacuole. The Rpl7a-GFP fusion is known to accumulate in the nucleus if treated with diazaborine (Pertschy et al., 2004). Thus, if the treatment with a potential inhibitor leads to the accumulation of the GFP signal in the nucleolus and/ or the nucleus, this suggested an inhibition of the ribosome biogenesis. Moreover, the temporal component was evaluated throughout the time series. The cells were treated with the potential inhibitors, using either the determined MIC or empirical values (see master thesis Dominik Awad), if no MIC was determined. To exclude any effects of the solvent DMSO, an appropriate volume was added to the untreated control cells. The wildtype C303a strain was investigated under the same conditions to check if the potential inhibitor itself exhibits a

florescence signal. In case of background fluorescence, the compound was unsuitable for this screen.

Upon treatment with 40 µM acivicin, an accumulation of the fluorescence signal in the nucleolus was observed (figure 3). After 60 min, an accumulation in the nucleolus was visible and became more pronounced after 90 min of treatment. After shorter treatment periods than 60 min, the distribution of the fluorescence signal did not differ from the untreated cells and there was also no difference between 90 and 120 min of treatment. No autoflorescence was observed for this compound.

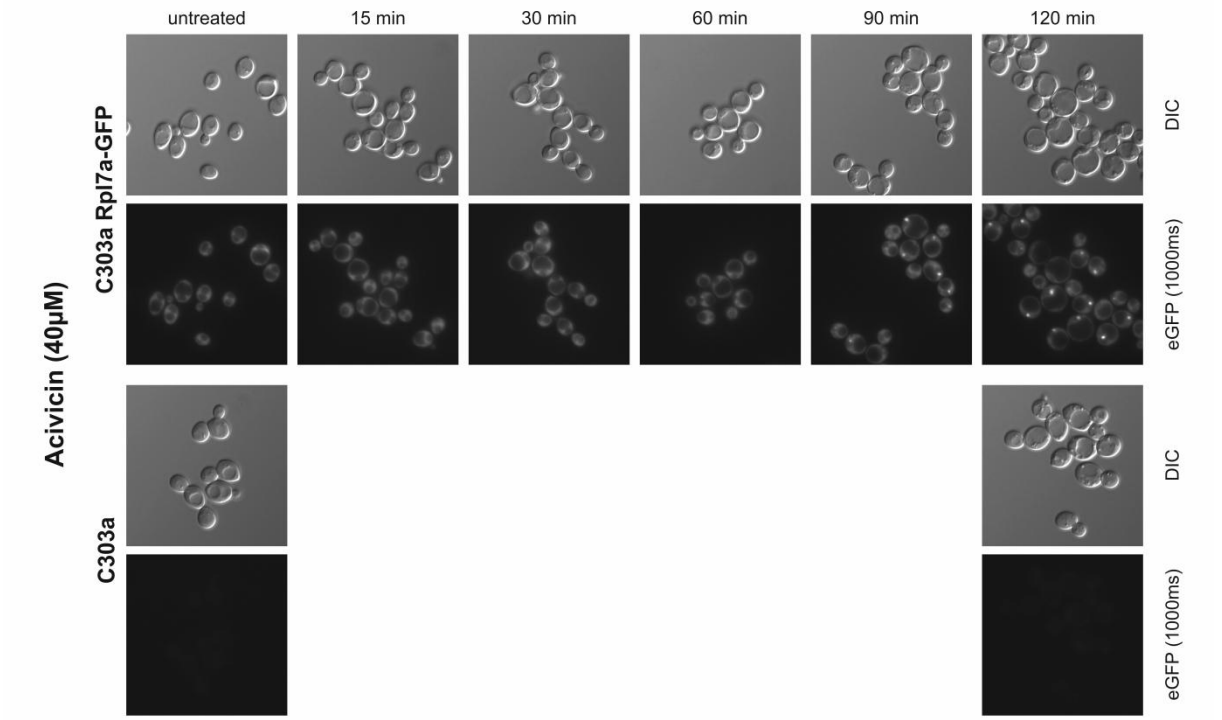

Figure 3: Time series of the potential inhibitor acivicin (40 µM). After 60 min of treatment, a faint accumulation in the nucleolus of the C303a Rpl7a-GFP strain is visible, whereas after 90 min it gets more distinct. No fluorescence of the compound itself is observed in the wildtype strain C303a.

An accumulation of the GFP signal in the case of carmofur (60 µM) was observed in the time scale from 180 min to 360 min (figure 4), whereas the accumulation in the nucleolus was not as distinct as compared to acivicin. Before 180 min of treatment, no effects on the distribution of the Rpl7-GFP fusion protein were observed. The images of the treated wildtype strain C303a did not indicate a fluorescence of the compound itself.

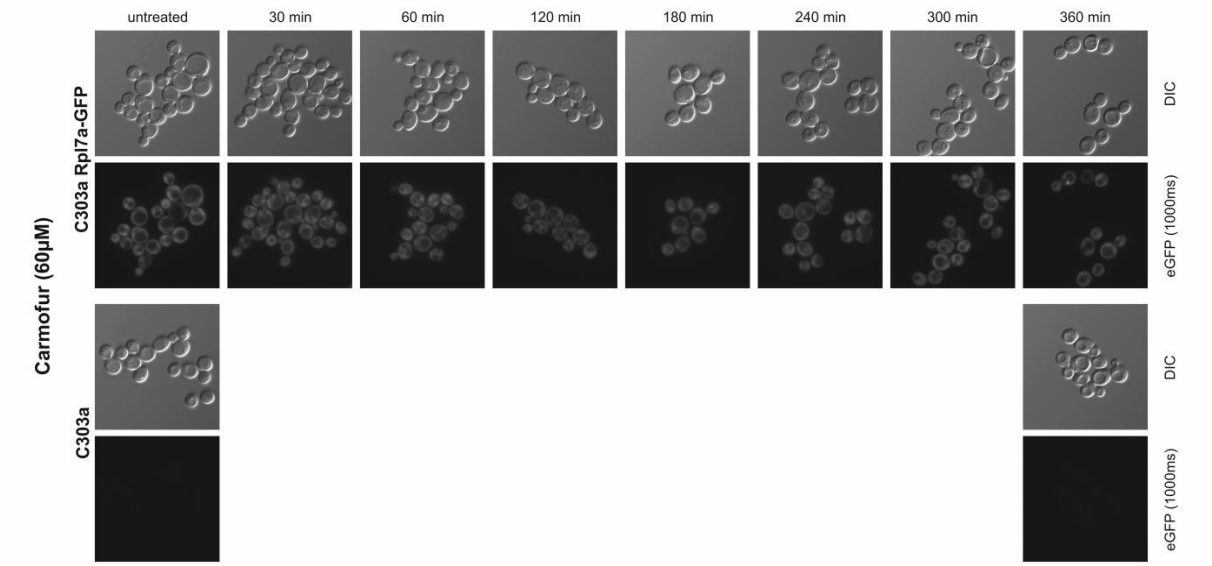

Figure 4: Time series of the potential inhibitor carmofur (60 µM). Accumulation of the GFP-signal in the nucleolus is observed from 180 min on in the C303a Rpl7a-GFP strain. The treatment of the wildtype C303a strain does not indicate a fluorescence of the inhibitor itself.

When the C303a Rpl7a-GFP cells were incubated with 60 µM curcumin, the GFP signal seemed to be enhanced after 30 min and no evaluation of an accumulation was possible (figure 5). After 90 min of treatment, the observed effect weakened. However, the investigation of the C303a wildtype strain revealed that the fluorescence arose from the compound itself. Hence, the observed effect was attributed to the autofluorescence of curcumin and no statement concerning an accumulation was possible.

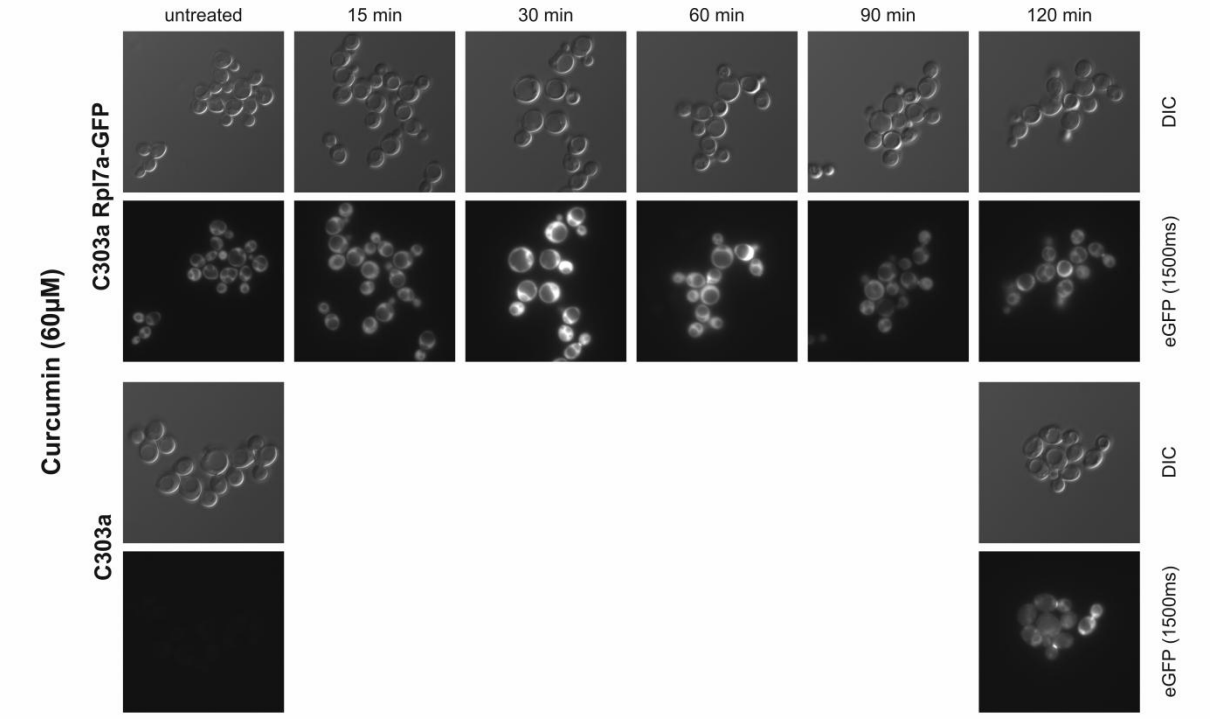

Figure 5: Time series of the potential inhibitor curcumin (60 µM). After 30 min of treatment, an enhanced GFP-signal is observed in the C303a Rpl7a-GFP strain, which weakens over time. The effect is attributed to the autofluorescence of curcumin, which was found by examining the wildtype C303a strain. No statement concerning a possible inhibition of ribosome biogenesis is possible.

The treatment of the Rpl7-GFP cells with 200 µM epirubicin lead to an accumulation of the fluorescence signal in the nucleolus after 90 min (figure 6). After shorter treatment periods, no effect upon treatment was observed. The investigation of the C303a cells did not show a fluorescence of the potential inhibitor itself.

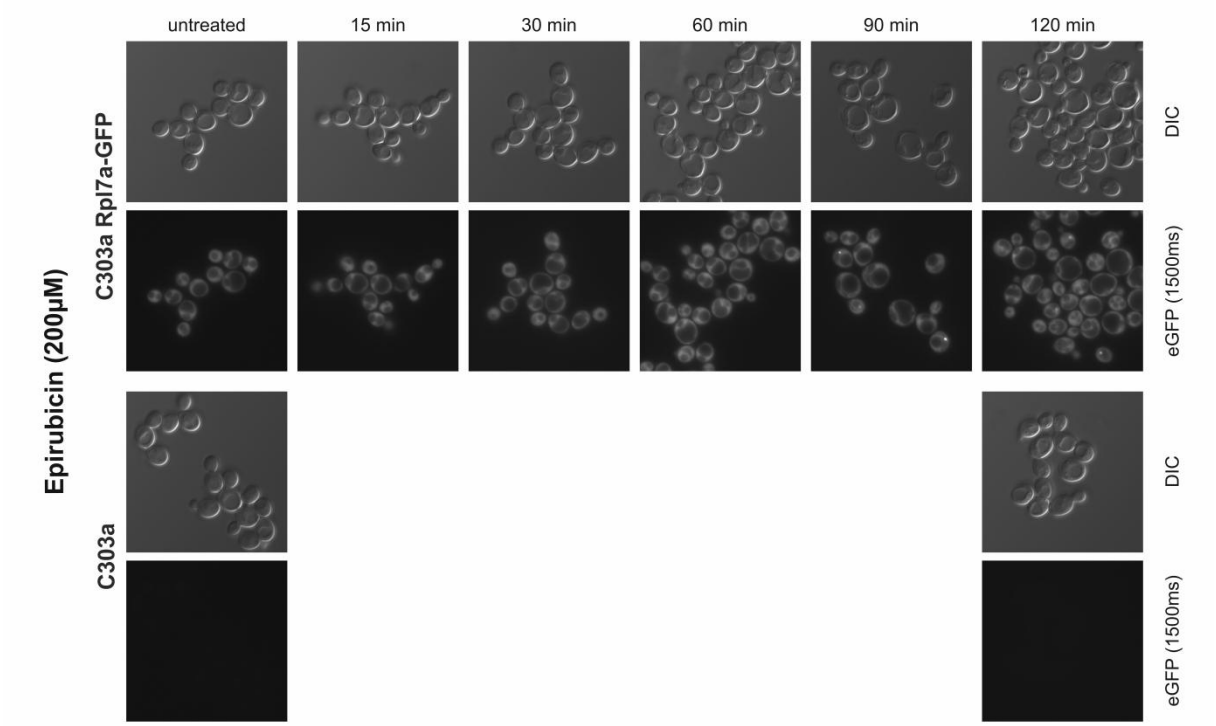

Figure 6: Time series of the potential inhibitor epirubicin (200 µM). An accumulation of the GFP signal in the nucleolus is observed at 90 min and 120 min of treatment. At shorter treatment periods, no effect is visible. A fluorescence of epirubicin itself is excluded by investigation of the treated C303a cells.

C303a Rpl7a-GFP cells, which were treated with 60 µM mycophenolic acid, showed an accumulation of the fluorescence signal in the nucleolus after 60 min (figure 7). After shorter treatment period (0-30 min) the localisation of the GFP fusion protein did not differ from the untreated control. The investigation of the treated C303a cells did not indicate a fluorescence of the compound itself.

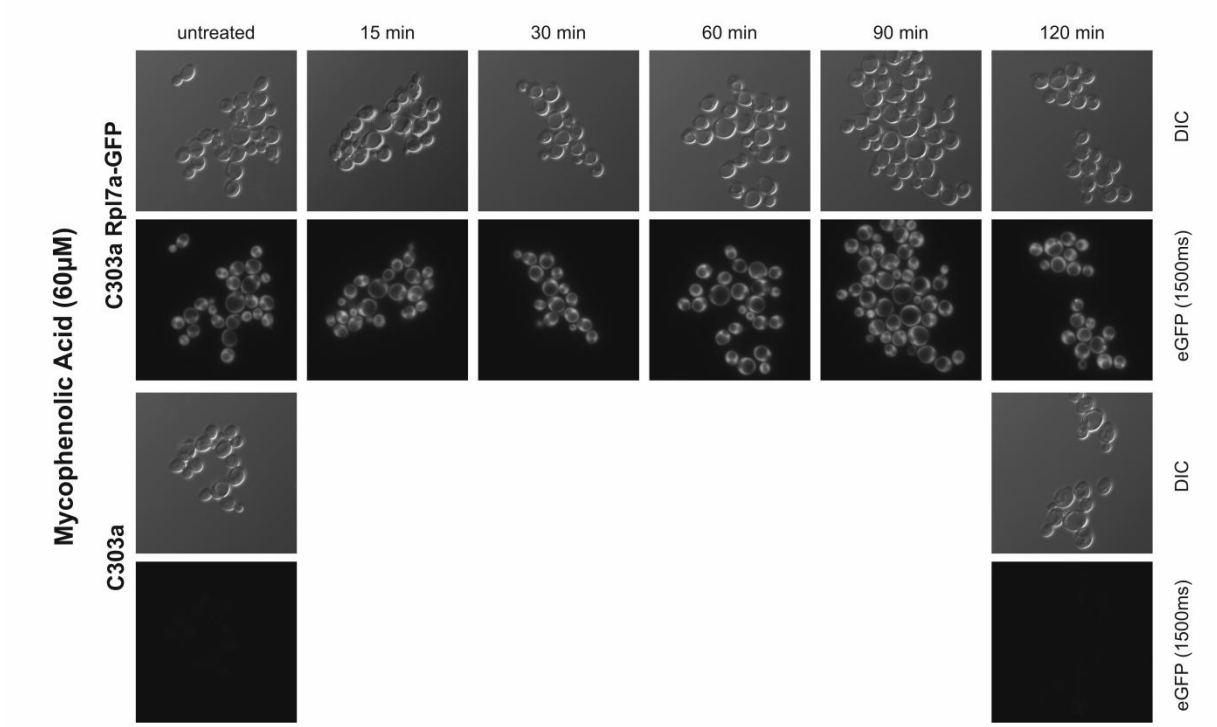

Figure 7: Time series of the potential inhibitor mycophenolic acid (60 µM). Upon treatment of the C303a Rpl7a-GFP cells with the compound, an accumulation in the nucleolus after 60 min is observed. Shorter incubation with mycophenolic acid does not show an alteration of the GFP signal. In this case background fluorescence is excluded due to the investigation of treated C303a cells.

In the case of usnic acid (40 µM) an accumulation of Rpl7a-GFP in the nucleus was obvious already after 15 min of treatment (figure 8). After 30 min it was more distinct and after longer treatment periodes the cytoplasmic signal became weaker. The investigation of treated C303a cells did not show an autoflorescence.

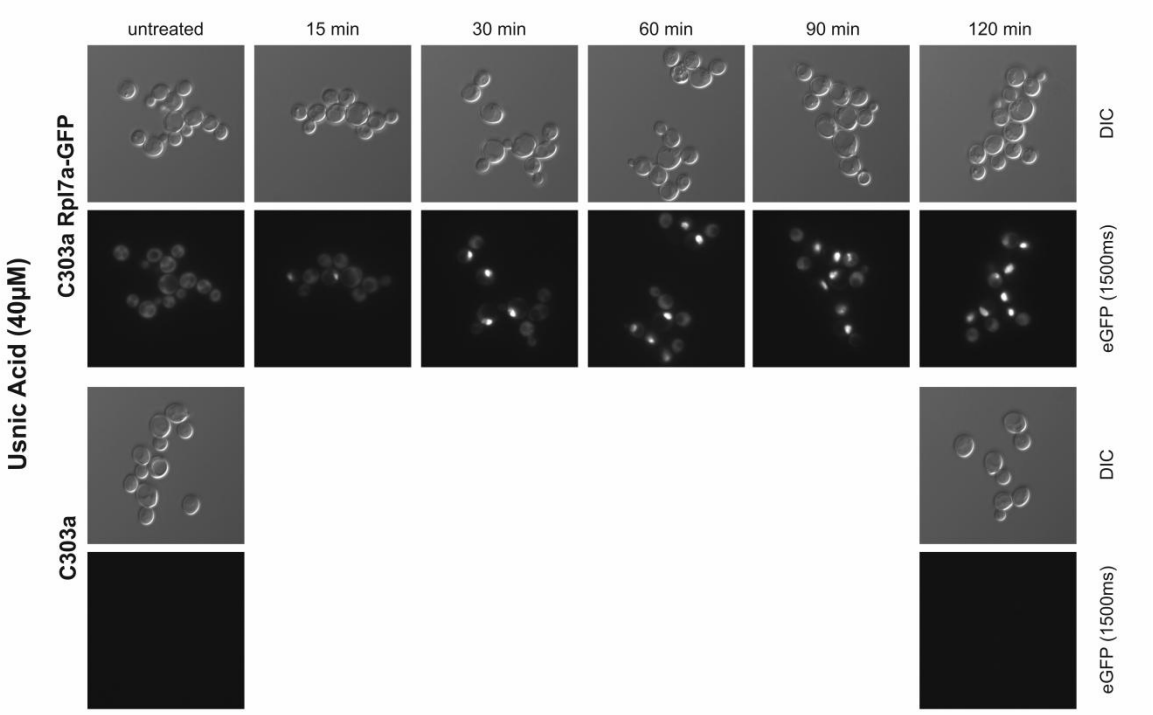

Figure 8: Time series of the potential inhibitor usnic acid (40 µM). Already after 15 min the accumulation of the GFP signal in the nucleus is observed. Over time, the signal alters, as the cytoplasmic signal weakens. A fluorescence of the inhibitor itself is excluded by investigation of treated C303a cells.

The accumulation of the fluorescence signal in the case of usnic acid was visible already after 15 min. Hence, the timescale between 0 and 15 min was investigated in more detail (figure 9). For this purpose, every two minutes after addition of 40 µM usnic acid a picture of the same image section was taken. It was noticed that already after 2 min a faint accumulation of Rpl7a-GFP in the nucleus was visible and after 4 min the accumulation was more pronounced.

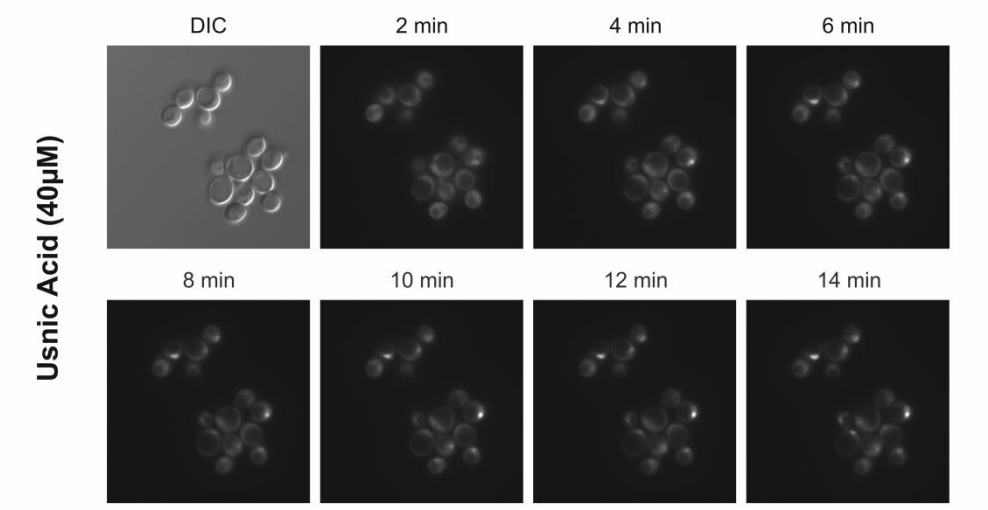

Figure 9: Short time series of the potential inhibitor usnic acid (40 µM). After addition of the compound a picture is taken from the same image section every 2 min. A faint accumulation of Rpl7a-GFP in the nucleus is detectable after 2 min and becomes more pronounced after longer treatment periods.

The treatment of C303a Rpl7a-GFP cells with 300 µM vulpinic acid did not lead to an accumulation of the signal in the nucleolus or the nucleus (figure 10). However, a reduction of the GFP-signal in the cytoplasm was observed after 15 to 360 min of treatment. The treated C303a strain without GFP tagged Rpl7a showed a faint fluorescence after incubation for 6 h with the potential inhibitor, suggesting that the compound or a product thereof showed a significant autofluorescence.

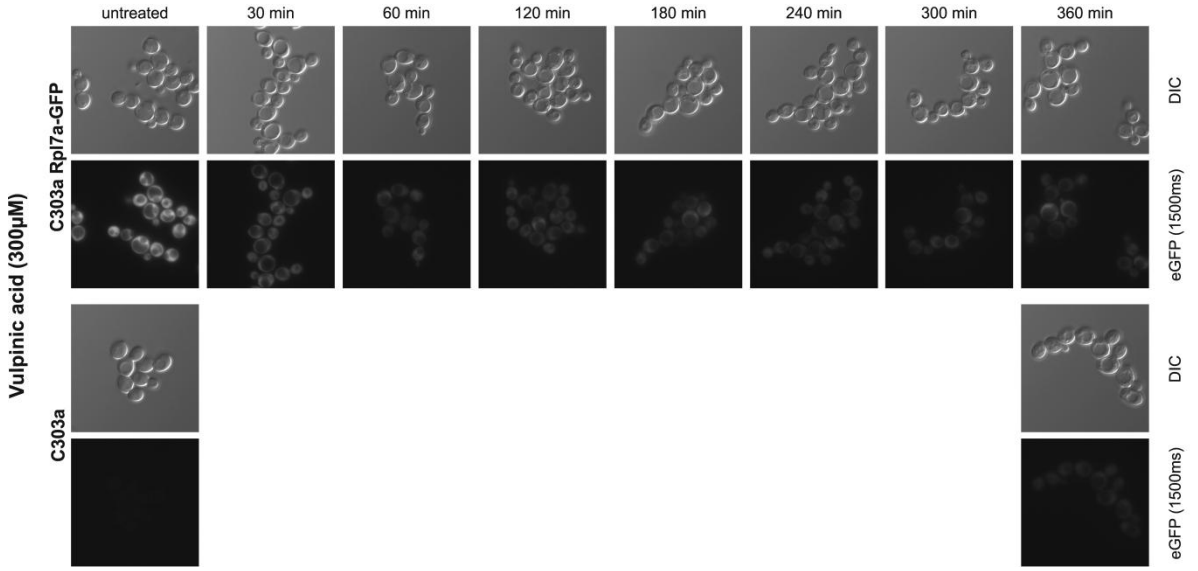

Figure 10: Time series of the potential inhibitor vulpinic acid (300 µM). A reduction of the cytoplasmic GFP signal is observed upon treatment of the C303a Rpl7a-GFP cells. However, after 6 h of treatment of the untagged C303a a faint fluorescence was observed, suggesting that the compound or a product thereof exhibits autofluorescence.

3.3. Efforts to identify the target of usnic acid

The determination of the MIC and the investigation in a microscopic time series provided the basic information to select the most promising potential inhibitor for the identification of the exact target of the compound. Mycophenolic acid and vulpinic acid were unsuitable as no MIC was determined and curcumin was excluded as no accumulation was confirmed due to the autofluorescence of the inhibitor. From the four remaining compounds, usnic acid was chosen, since the treated C303a Rpl7a-GFP cells showed the fastest accumulation of the GFP fusion protein in comparison to acivicin, carmofur and epirubicin. Moreover, usnic acid was the only compound showing an accumulation of the GFP signal in the nucleus.

3.3.1. Generation of a resistant mutant

The starting point for the construction of a gene library was the identification of a suitable yeast mutant, which was resistant to the potential inhibitor usnic acid. In order to receive a

reasonable mutation rate, the UV radiation dose for a 50% survival rate was figured out by determination of the mortality rate at various UV doses (figure 11).

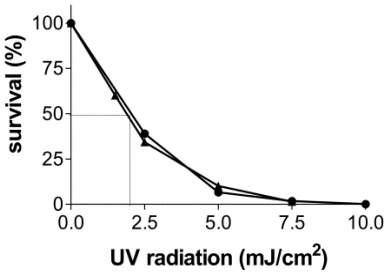

Figure 11: Mortality curve of UV irradiated C303a Δyap1. Two times, the colonies after UV irradiation were counted and converted to a survival in percent (%), whereas the unirradiated sample was set as 100%. The point at which the mortality rate was 50% was calculated with linear regression.

At an UV radiation dose of 2 mJ/cm^2 the mortality rate was 50%, hence this dose was used for randomly mutating C303a Δyap1 cells. These cells were then screened by a spotting assay for mutants, which showed resistance to usnic acid. In addition to the growth on SD+all and SD+all+80 µM usnic acid plates, the growth on YPD, YPD+0.5 µg/ml cycloheximide, YPD+0.25 µg/ml 4-nitroquinolin N-oxid (4-NQO) was examined, since the resistance to usnic acid could also be due to a multi-drug-resistance. As in the first spotting assay, many false positives had been identified, only a few mutants were tested in a second spotting test (figure 12). On YPD two of the mutants (22a and 37) showed a slight growth defect in comparison to the C303a Δyap1 strain, whereas on SD+all medium this difference in growth was hardly visible. These two mutants also showed a slight growth on YPD+0.25 µg/ml 4-NQO in contrast to all other spotted strains. Moreover, on YPD+0.5 µg/ml cycloheximide, the same two mutants grew, suggesting a multi-drug-resistance mechanism. Only the mutants 22a and 22b showed a clear growth on SD+80 µM usnic acid medium. Hence, 22b was the only mutant that showed the desired phenotype and was therefore chosen for further investigations.

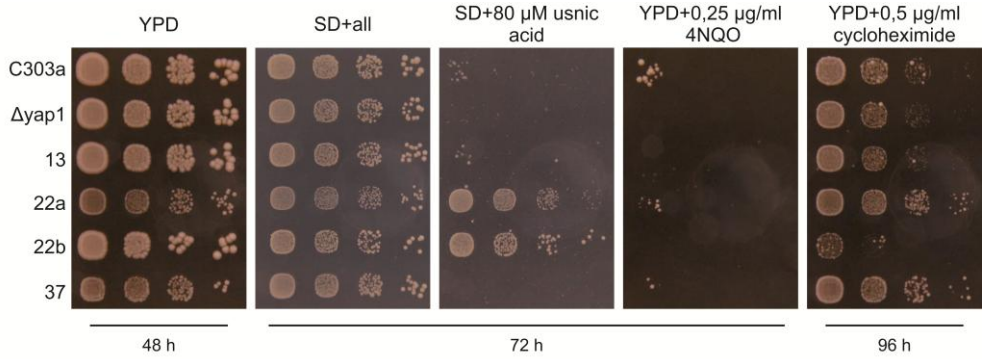

Figure 12: Spotting assay for identification of mutants resistant to usnic acid. The focus at this spotting assay is on distinguishing mutants only resistant to usnic acid from false positives showing a multi-drug-resistance phenotype, thus showing also growth on YPD+0.25 µg/ml 4-NQO and YPD+0.5 µg/ml cycloheximide. The C303a and the Δyap1 strain serve as growth control. Just the mutant 22b shows the desired phenotype.

3.3.2. Construction of a representative gene library

For gene library construction, the isolated genomic DNA of the mutant 22b was fragmented by partial digestion with Bsp143I with the aim to obtain a maximum amount of fragments with a length of 3 to 10 kb. At this range of size, each insert was supposed to contain about 1 to 3 genes assuming that the DNA was randomly fragmented. The optimal digestion time was determined by a pilot experiment (figure 13). The maximum amount of fragments with the desired length distribution was obtained between digestion for 25 and 30 min and thus the genomic DNA was digested for 27.5 min for the main experiment.

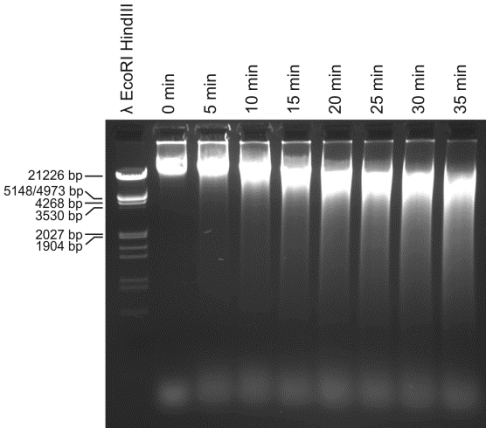

Figure 13: Partial digestion of genomic DNA with Bsp143I. Genomic DNA was digested for different periods of time with the aim to obtain a maximum amount of 3 to 10 kb fragments.

The partial digested DNA was fractioned as described in the methods section (2.10.3. Fractionation of genomic DNA fragments) and the purified DNA fragments were examined on a gel (figure 14). By pooling fractions 6 to 11, it was ensured, that no fragments smaller than 3bp or larger than 10 kb were used for ligation with the vector pRS316.

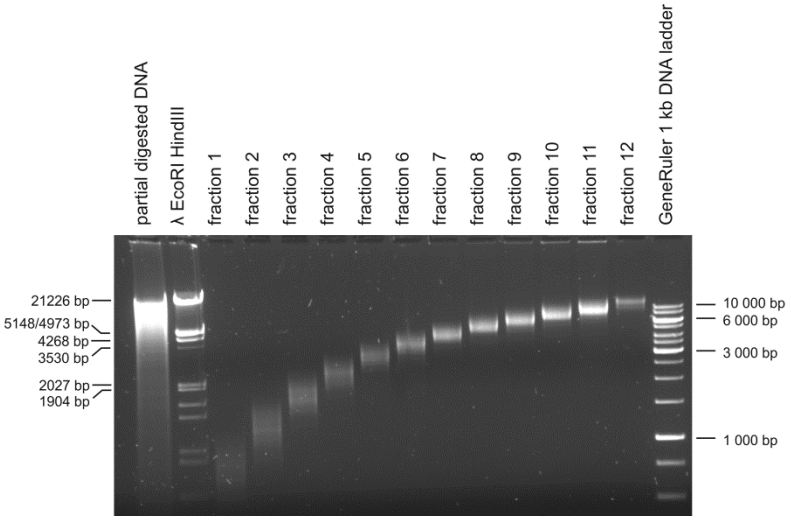

Figure 14: Fractions of partial digested DNA. The fractions 6 to 11 were pooled and used for ligation with pRS316. This strategy should lead to an insert size range of approximately 3 to 10 kb.

The ligated gene library plasmids were transformed in *E. coli*, yielding approximately 16500 transformants. Since yeast has about 6100 genes and it was assumed, that in average 2 genes were found on each insert, every gene ought to be present in the pool of transformants. The plasmids were isolated from *E. coli* and the gene library was examined for its representativity.

Initially, an uncleaved and a NotI cleaved aliquot of the gene library plasmids were visualised on an agarose gel (figure 15A). In the lane of the uncleaved plasmids the detected sizes ranged from approximately 1000 bp to over 21000 bp. For estimation of the insert size, the NotI cleaved aliquot and hence linearised gene library plasmids were examined. The dominant and diffuse band above 5000 bp indicated that there were inserts ligated, since the vector backbone had a size of 4887 bp. Due to the ligation of fractioned DNA fragments, the plasmid sizes ranged in a narrow range. The fainter band at the size of 5000 bp indicated the amount of religated vector, which account for one tenth of the isolated plasmids. However, also smaller fragments were detected, which were believed to be degradation products originating from the isolation.

To test, wether the gene library was representative, it was screened for three genes *DRG1*, *NUP116* and *NUP159* by PCR. Amplificats of these three genes were detected at the adequate heights of 2343 bp, 2222 bp and 2211 bp (figure 15B). Hence it was suggested that if these genes were present the gene library, it was representative.

Furthermore, the W303a strain was transformed with an aliquot of the gene library plasmids, showing a transformation rate of $1.3 \cdot 10^4$, to investigate the frequency of the *ADE2* and the *HIS3* gene. The smaller *HIS3* (1347bp) was found in 5 of $1.4 \cdot 10^4$ transformants, whereas the slightly larger *ADE2* (1716 bp) was not found in $1.4 \cdot 10^4$ transformants.

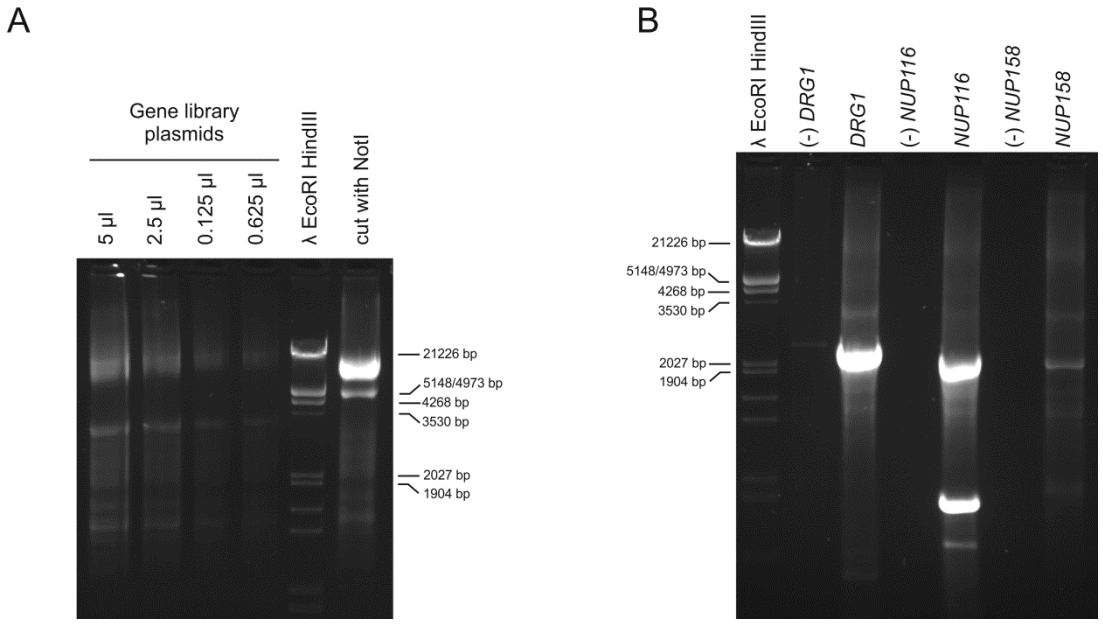

Figure 15: Investigating the representativity of the isolated gene library plasmids. A) The uncleaved plasmids were detected in a smear. Concerning the insert size, the NotI cleaved and thus linearised gene library plasmids have to be examined. The diffuse, but dominant band above 5000 bp shows that DNA fragments of a certain size, which were determined by fractionation, have been ligated, since the vector backbone consists of 4887 bp. The fainter band at 5000 bp shows the amount of religated vector. The fragments detected beneath 5000 bp are believed to be degradation products originating from the isolation. **B)** Via PCR the gene library plasmids were searched for *DRG1*, *NUP116* and *NUP158* and the adequate amplificats are observed at 2343 bp, 2222 bp and 2211 bp. Hence, it is suggested that the gene library is representative.

3.3.3. Attempts to identify the gene providing resistance to usnic acid

The obtained gene library generated from the resistant mutant was transformed in the C303a Δyap1 strain, to find the allelic form of the gene responsible for resistance to usnic acid and thus identify the target of the compound. For each transformation 4 µl of the gene library plasmid were used. In the first attempt, the cells were directly plated on SD-ura+80 µM usnic acid for selection on the plasmid and simultaneously screening for resistant transformants. Comparison between the control and the screened cells showed, that approximately one tenth of the transformant, which obtained a plasmid, were able to grow on usnic acid. Since this ratio was unreasonable, in the next attempt, the cells were first selected for the gene library plasmid on SD-ura plates and were then replicaplated on SD-ura+80 µM usnic acid plates. Thus, 16 out of the $5 \cdot 10^3$ screened transformants showed a better growth than the rest. These transformants were further investigated in a spotting assay to examining their resistance to usnic acid and the phenotype of multi-drug-resistance. However, none of the tested tranformants showed an usnic acid resistant phenotype that could indicate the presence of the searched mutated gene.

3.4. Investigation of early pre-60S particle by TAP purification

Besides the genetic approach for the identification of the target of the potential inhibitor usnic acid, the effect of this compound on the early 60S subunit maturation was investigated by TAP purification. Our preliminary results showed a 27SA2 pre-rRNA accumulated upon usnic acid treatment of yeast cells, indicating that a very early step in large subunit is blocked by the compound. To investigate the effect of the compound on early pre-ribosomal particle formation, we isolated pre-60S particle using Noc2-TAP as bait protein, which co-purifies the 27SA2 pre-rRNAs and the downstream products 27SA3 and 27SB. A perturbation of ribosome biogenesis by usnic acid should thus be obvious by a change in the particle composition. The crude extracts and the TEV eluates with the purified pre-ribosomal particles from treated and untreated cells were analysed by SDS PAGE and subsequent coomassie staining and western blotting.

The coomassie stained gel was used for the validation of the purification and the investigation of alterations of the protein pattern in the TEV eluates (figure 16A upper part). However, no striking differences were observed by comparison of the usnic acid treated with the untreated sample. The investigation by western blotting validated the purification of the particles, as in the lanes of the crude extracts no or only a weak signal was detected, in contrast to the lanes of the TEV eluates were distinct bands for early maturation factors were detected (Figure 16A lower part). The bait protein, which was detected using the Cbp antibody, showed a slightly stronger signal in the lane of the TEV eluate from the treated cells than of the untreated control. This indicated that in this lane more protein was loaded onto the gel. Hence, an increase in protein level to a similar extent, as observed in the case of Noc1, Nog1, Rpl5 and Rpl16, suggested that the level of these proteins did not change due to the treatment. In contrast, a reduction of the signal and thus of the protein amount was observed for Noc3, Rrp12 and Rpa135 in the pre-ribosomes from the treated cells.

The finding concerning the reduction of Rpa135 was supported by the result of the mass spectometric analysis of a Noc2-TAP purification. On the coomassie gel slight differences in the intensity of 4 bands were identified and thus, the proteins were identified by mass spectometry (figure 16B). Beside the heat shock protein Ssb2 and the cytoplasmic co-chaperone Sgt2, the RNA polymerase subunit Rpa135 and nuclear protein Pno1, which is required for pre-18S rRNA processing, were identified. The alteration in the intensity of the

protein bands indicated a decrease in the amount of Rpa135 upon treatment and an increase of Ssb2, Sgt2 and Pno1.

These results in combination with the outcome of the northern blot (Mathias Loibl, unpublished data; figure 16C) provided more details concerning the possible target of usnic acid. First, the decrease of the 35S rRNA observed by northern blotting is consistent with the decrease of Rpa135 and of the very early acting pre-ribosome maturation factor Rrp12 (Moriggi G, 2014) after usnic acid treatment. In addition the observed decrease of Noc3, which binds at a later maturation step in the nucleolus, is consistent with the accumulation of 27SA2 pre-rRNA and the decrease of 7S pre-rRNA in treated cells as observed by northern blotting.
Taken together, these results suggest that the target of usnic acid or at least its effects on pre-60S biogenesis affects a maturation step, where Noc1 is bound to Noc2, but Noc3 has not yet joined the particle and where the 27SA rRNA is not yet processed to the 27SB rRNA. Thus, this phase should be the focus of further investigations.

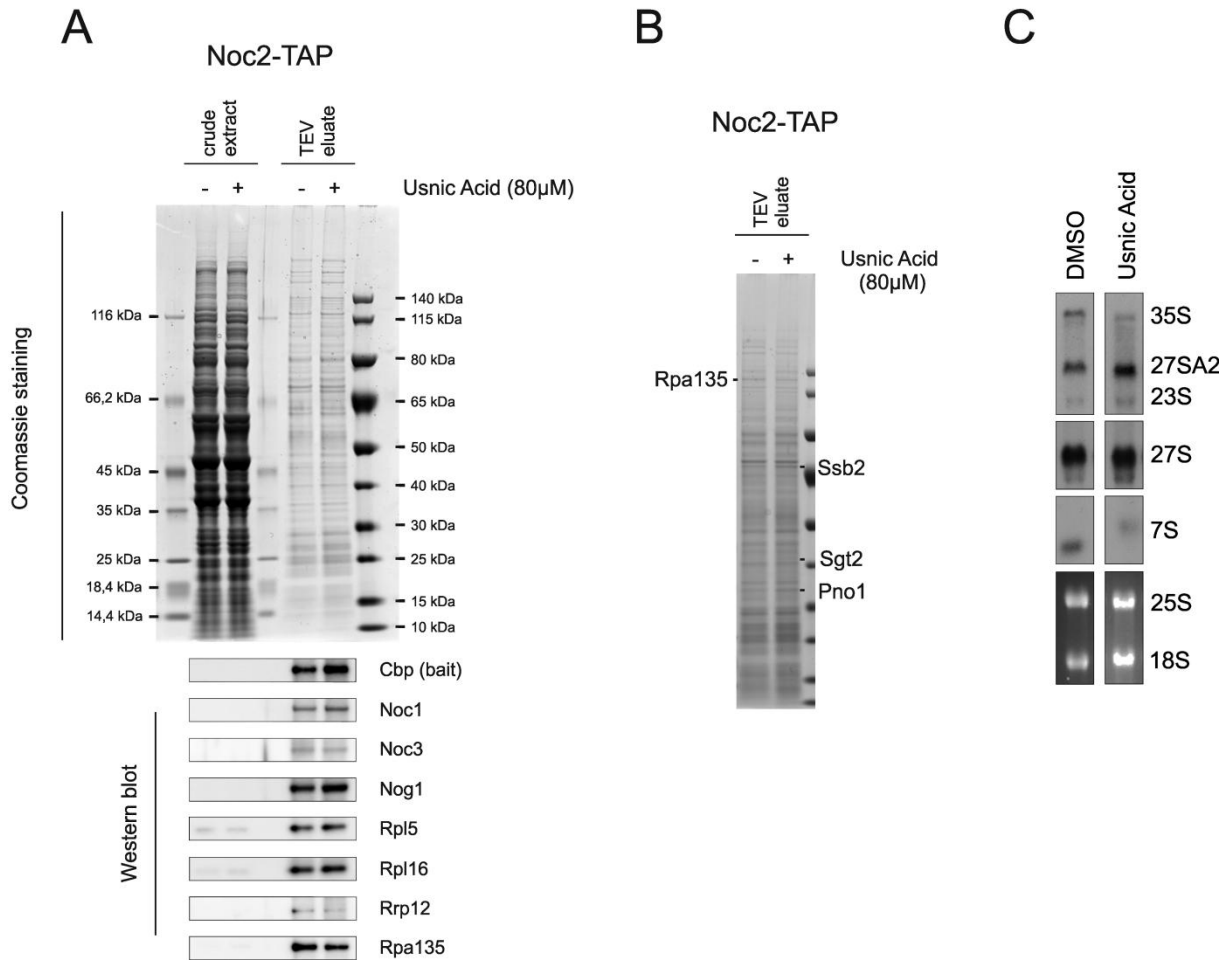

Figure 16: Effect of usnic acid on early pre-60S particle composition and the rRNA. A) TAP purification of early pre-60S particles using Noc2-TAP treated with usnic acid (80 µM) for 30 min. The comparison of the TEV eluate lanes of the untreated (-) and the treated (+) samples does not show pronounced alterations of the protein pattern. The detection of the bait protein Noc2 with the Cbp antibody in the western blot indicates that in the lane of the treated sample, more protein was loaded (lower part). By considering this quantitative difference, the amount of Noc1, Nog1, Rpl5 and Rpl16 is not altered by the treatment with usnic acid. In the case of Noc3, Rrp12 and Rpa135 the ratio of the untreated to treated signal changes in comparison to the bait protein, since the signal is weaker in the lane of the TEV eluate of the treated sample. **B) Coomassie stained SDS-PAGE of Noc2-TAP TEV eluates with or without usnic acid treatment for mass spectometry.** For identification of possible differences in protein composition, a SDS-PAGE of a Noc2-TAP purification with more equal loading was used. The bands showing a different protein level in the treated compared to the untreated control are marked and the identified proteins indicated. Upon treatment the amount of the RNA polymerase I subunit Rpa135 was decreased, whereas the amount of heat shock protein Ssb2, the cytoplasmic co-chaperon Sgt2 and the nuclear protein Pno1, which is required for 18S rRNA processing, was increased. C**) Northern blot showing the effect of usnic acid on total rRNA composition.** By comparison of the untreated control (DMSO) with the usnic acid treated sample, a reduction of 35S rRNA can be observed. Furthermore, the 27SA2 rRNA accumulates in the treated cells, whereas the total amount of 27S rRNA remains unchanged indicating a decrease of the 27SB rRNA. Consistent with this view, the amount of 7S rRNA is also decreased. The 25S and 18S rRNA served as loading control (taken from Mathias Loibl, unpublished data).

4. Discussion and Outlook

The aim of this study was the characterisation of several potential inhibitors and to track down the target of the most promising compound. The basic information was provided by determination of the MIC and by the microscopic investigation of the inhibition of the ribosome biogenesis. These data is useful for further experimental approaches, moreover it could provide explanations for future findings. Based on these initial characterisations, usnic acid was chosen to be the potential inhibitor, who´s target should be identified.

Usnic acid (2,6-Diacetyl-7,9-dihydroxy-8,9b-dimethyldibenzofuran-1,3(2H,9bH)-dione) was first isolated by Knop (1844) and first synthesized by Curd and Robertson (1933). The substance is a yellow cortical pigment and occurs in two enantiomeric forms differing in the orientation of the angular methyl group at the position 9b. In nature, usnic acid is found in several lichen species, whereas closely related compounds have been found in some fungi (Ingólfsdóttir, 2002).

Many lichens containing usnic acid and their extracts have been used as crude drugs for a long time throughout the world for medicinal, perfumery, cosmetic and ecological applications. The pure substance has been added to creams, toothpaste, mouthwash, deodorants and sunscreen products and has been promoted for weight reduction. In some cases the purpose was the use as an active principle and in others as a preservative. In diverse studies it has been shown, that usnic acid exhibits antimicrobial, antiviral, antiprotozoal, antiproliferative, anti-inflammatory and analgesic activity, besides ecological effects, such as antigrowth, antiherbivore and anti-insect properties (reviewed in Ingólfsdóttir, 2002).

The various effects that are attributed to usnic acid might be the reason, why it became one of the most extensively studied lichen metabolites and its effects have been investigated in many studies. Thereof some examples should be mentioned in the following to show the diverse effects of this compound.

In mice, the excessive inflammatory response and oxidative stress in the lung tissue due to LPS-induced acute lung injury was suppressed by Usnic acid (Su et al., 2014).

In liver perfusion experiments the reported uncoupling activity concerning oxidative phosphorylation of usnic acid was confirmed at low concentrations. At higher concentrations, the effects obtained were among others the inhibition of the mitochondrial electron flow and the inhibition of medium-chain fatty acid oxidation. Thus, usnic acid was

classified as a narrow range uncoupler, as the characteristic effects of uncoupling were found in a concentration between 1 and 10 µM in rats (Moreira et al., 2013).

In cell culture studies, the triggering of autophagy by usnic acid was observed, whereas the degradation of the autophagosomal content was defective (Bessadottir et al., 2012). Another study suggested that usnic acid perturbed various interrelated signaling pathways and that autophagy was a defensive mechanism (Chen et al., 2014).

Others stated, that the cytotoxicity observed upon treatment with usnic acid was specific to cancer cells (HT29 cells), while non-cancer cells (MDCK cells) were not severely damaged (Nguyen et al., 2014).

Although many effects are associated with usnic acid treatment, the molecular mechanism is yet unknown. Only one study stated the cell membrane as the main target of usnic acid (Suwalsky et al., 2015).

Concerning the antifungal property of usnic acid, the study of Nithyanand et al. (2015) should be mentioned as an example. Although usnic acid did not exhibit any antifungal activity against *Candida albicans* (*C. albicans*) usnic acid decreased the viability of *C. albicans* significantly during its biofilm phase in a concentration dependent manner. The significant biofilm inhibition and the prevention of proper adhesion by usnic acid were caused by impairment of hyphal development.

In addition to the antiviral effect of usnic acid on the Herpes simplex type 1 virus, polio type 1 virus, genital human papillomavirus and the Epstein-Barr virus (Ingólfsdóttir, 2002), usnic acid also inhibited the proliferation of the mouse polyomavirus (Shtro et al., 2014). Campanella et al. (2002) stated that the antiviral activity could be the consequence of the drastic inhibition of RNA transcription and thus, this study mentioned a possible mechanism of action.

The results of studies investigating the antimicrobial properties of usnic acid also point towards perturbation of RNA and/or DNA synthesis. It has been demonstrated that usnic acid caused a rapid and strong inhibition of RNA and DNA synthesis in gram-positive bacteria (e.g. *Bacillus subtilis* and *Staphylococcus aureus*). The inhibitory effect on the protein synthesis was suggested to be indirect, possibly through impairment of transcription. On the contrary, no inhibition of DNA, RNA or protein synthesis was observed in *Escherichia coli*. However, in the gram-negative bacterium *Vibrio harveyi*, a slight inhibition of RNA synthesis was observed (Maciąg-Dorszyńska et al., 2014).

In general, it was stated, that usnic acid showed antimicrobial activity against gram-positive bacteria and mycobacteria, but not against gram-negative bacteria (reviewed Ingólfsdóttir, 2002).
In this context, a study showing the binding affinity of usnic acid to DNA has to be mentioned (Plsíkova et al., 2014). Furthermore, usnic acid acted on bacterial biofilms as shown in a study with *Streptococcus pyogenes* (Nithyanand et al., 2015).
Taken together, these studies indicated diverse effects upon treatment with usnic acid on various model systems. But these observations did not lead to the elucidation of the molecular mechanism or target respectively. At this point the consideration of Cardarelli et al. (1997) should be mentioned, as they suppose that "the substance acts in a similar way on cells of both animal and plant origin, probably by interfering with some key steps in cell division shared by such different cells".

This consideration could be consistent with our finding that usnic acid interferes with ribosome biogenesis, which is a highly conserved process, tightly linked to cell growth and thus cell division, assuming that the mechanism is the same in all organisms. Moreover, our observation of the decrease of the 35S rRNA in the northern blot upon usnic acid treatment goes along with the studies showing an inhibition of RNA synthesis. However, a global inhibition of RNA synthesis cannot explain the observed accumulation of 27SA2 pre-rRNA. Our TAP purifications showed that treatment with usnic acid lead to Noc2-containing pre-60S particles with decreased levels of Noc3 and RNA polymerase subunit Rpa135. The finding of reduced levels of Rpa135 are possibly related to the general decrease of 35S pre-rRNA observed in total RNA preparations by northern blotting. However, if the decrease of 35S pre-rRNA and the accumulation of 27SA2 pre-rRNA are really directly related cannot be answered based on the available data. This question could be answered by the identification of the exact target using the genetic approach of a gene library based on a resistant mutant. Therefore it is important to follow up the results of this study, which suggest methodical improvements, for instance regarding the preparation of the usnic acid agar plates used for the screening. Especially, the insolubility of usnic acid in water provided serious problems. Although the compoind is solubilised in DMSO, the addition to agar might lead to precipitation of usnic acid. Concerning this problem, the usage of the potassium salt of usnic acid (potassium usnate) could be an option. The conversion is fast and easy and the solubility in water of potassium usnate was stated to be increased (100%) without losing its biological activity (Martins et al., 2014).

Moreover, one should consider if the generation of a new resistant mutant would be helpful, as the one used in this study was found to be sterile. The mating of the resistant mutant would permit the crossing back with the wildtype, which would be an advantage.

Taken together, this study shows a possible strategy for the characterisation of novel identified possible inhibitors and an experimental approach for the identification of the exact target.

5. References

Andrews JM, 2001: *Determination of minimum inhibitory concentrations.* J Antimicrob Chemother. 48 Suppl 1:5-16.

Bessadottir M, Egilsson M, Einarsdottir E, Magnusdottir IH, Ogmundsdottir MH, Omarsdottir S and Ogmundsdottir HM, 2012: *Proton-shuttling lichen compound usnic acid affects mitochondrial and lysosomal function in cancer cells.* PLoS One. 7:e51296.

Burger K, Mühl B, Harasim T, Rohrmoser M, Malamoussi A, Orban M, Kellner M, Gruber-Eber A, Kremmer E, Hölzel M and Eick D, 2010: C*hemotherapeutic drugs inhibit ribosome biogenesis at various levels.* J Biol Chem. 285:12416-25.

Campanella L, Delfini M, Ercole P, Iacoangeli A and Risuleo G, 2002: *Molecular characterization and action of usnic acid: a drug that inhibits proliferation of mouse polyomavirus in vitro and whose main target is RNA transcription.* Biochimie. 84:329-34.

Cardarelli M, Serino G, Campanella L, Ercole P, De Cicco Nardone F, Alesiani O and Rossiello F, 1997: *Antimitotic effects of usnic acid on different biological systems.*Cell Mol Life Sci. 53:667-72.

Chen S, Dobrovolsky VN, Liu F, Wu Y, Zhang Z, Mei N and Guo L, 2014: *The role of autophagy in usnic acid-induced toxicity in hepatic cells.* Toxicol Sci. 142:33-44.

Curd FH, Robertson A and Stephenson R, 1933: *40. Lichen acids.* Part IV. Atranorin. J Chem Soc. 0:130–3.

Gietz RD, 2014: *Yeast transformation by the LiAc/SS carrier DNA/PEG method.* Methods Mol Biol. 1163:33-44.

Harnpicharnchai P, Thongaram T, Sriprang R, Champreda V, Tanapongpipat S and Eurwilaichitr L, 2007: *An efficient purification and fractionation of genomic DNA from soil by modified troughing method.* Lett Appl Microbiol. 45:387-91.

Hurt E, Hannus S, Schmelzl B, Lau D, Tollervey D and Simos G, 1999: *A novel in vivo assay reveals inhibition of ribosomal nuclear export in ran-cycle and nucleoporin mutants.* J Cell Biol. 144:389-401.

Ingólfsdóttir K, 2002: *Usnic acid.* Phytochemistry. 61:729-36.

Kief DR and Warner JR, 1981: *Coordinate control of syntheses of ribosomal ribonucleic acid and ribosomal proteins during nutritional shift-up in Saccharomyces cerevisiae.* Mol Cell Biol. 1:1007-15.

Knop W, 1844: *Chemisch-physiologische Untersuchung über die Flechten.* Justus Lieb. Ann. Chem. (formerly Ann. Chem. Pharm.) 49, 103–124.

Loibl M, Klein I, Prattes M, Schmidt C, Kappel L, Zisser G, Gungl A, Krieger E, Pertschy B and Bergler H, 2014: *The drug diazaborine blocks ribosome biogenesis by inhibiting the AAA-ATPase Drg1*. J Biol Chem. 289:3913-22.

Maciąg-Dorszyńska M, Węgrzyn G and Guzow-Krzemińska B, 2014: *Antibacterial activity of lichen secondary metabolite usnic acid is primarily caused by inhibition of RNA and DNA synthesis.* FEMS Microbiol Lett. 353:57-62.

Martins MC, Silva MC, Silva LR, Lima VL, Pereira EC, Falcão EP, Melo AM and da Silva NH, 2014: *Usnic acid potassium salt: an alternative for the control of Biomphalaria glabrata (Say, 1818).* PLoS One. 9:e111102.

Moreira CT, Oliveira AL, Comar JF, Peralta R and Bracht A, 2013: *Harmful effects of usnic acid on hepatic metabolism.* Chem Biol Interact. 203(2):502-11.

Moriggi G, Nieto B and Dosil M, 2014: *Rrp12 and the Exportin Crm1 participate in late assembly events in the nucleolus during 40S ribosomal subunit biogenesis.* PLoS Genet. 10:e1004836.

Nguyen TT, Yoon S, Yang Y, Lee HB, Oh S, Jeong MH, Kim JJ, Yee ST, Crişan F, Moon C, Lee KY, Kim KK, Hur JS, Kim H, 2014: *Lichen secondary metabolites in Flavocetraria cucullata exhibit anti-cancer effects on human cancer cells through the induction of apoptosis and suppression of tumorigenic potentials*. PLoS One. 9:e111575.

Nithyanand P, Beema Shafreen RM, Muthamil S and Karutha Pandian S, 2015: *Usnic acid inhibits biofilm formation and virulent morphological traits of Candida albicans.* Microbiol Res. 179:20-8.

Nithyanand P, Beema Shafreen RM, Muthamil S and Karutha Pandian S, 2015: *Usnic acid, a lichen secondary metabolite inhibits Group A Streptococcus biofilms.* Antonie Van Leeuwenhoek. 107:263-72.

Pertschy B, Zisser G, Schein H, Köffel R, Rauch G, Grillitsch K, Morgenstern C, Durchschlag M, Högenauer G and Bergler H, 2004: *Diazaborine treatment of yeast cells inhibits maturation of the 60S ribosomal subunit.* Mol Cell Biol. 24:6476-87.

Piper P, 1996*: Isolation of Yeast DNA.* Yeast Protocols - Methods in Molecular Biology, Vol 53, chapter 11, edited by I Evans, Humana Press Inc , Totowa, NJ.

Plsíkova J, Stepankova J, Kasparkova J, Brabec V, Backor M and Kozurkova M, 2014: *Lichen secondary metabolites as DNA-interacting agents.* Toxicol In Vitro. 28:182-6.

Quin JE, Devlin JR, Cameron D, Hannan KM, Pearson RB and Hannan RD, 2014: T*argeting the nucleolus for cancer intervention.* Biochim Biophys Acta. 1842:802-16.

Rubbi CP and Milner J, 2003: *Disruption of the nucleolus mediates stabilization of p53 in response to DNA damage and other stresses.* EMBO J. 22:6068-77.

Sambrook J, Fritsch EF and Maniatis T, 1989: *Molecular Cloning: A Laboratory Manual.* 2nd ed. Plainview, N.Y.: Cold Spring Harbor Laboratory Press.

Shtro AA, Zarubaev VV, Luzina OA, Sokolov DN, Kiselev OI and Salakhutdinov NF, 2014: *Novel derivatives of usnic acid effectively inhibiting reproduction of influenza A virus. Bioorg Med Chem.* 22:6826-36.

Stokes JM and Brown ED, 2015: *Chemical modulators of ribosome biogenesis as biological probes. Nat Chem Biol.* 11:924-32.

Su ZQ, Mo ZZ, Liao JB, Feng XX, Liang YZ, Zhang X, Liu YH, Chen XY, Chen ZW, Su ZR and Lai XP, 2014: *Usnic acid protects LPS-induced acute lung injury in mice through attenuating inflammatory responses and oxidative stress.* Int Immunopharmacol. 22:371-8.

Suwalsky M, Jemiola-Rzeminska M, Astudillo C, Gallardo MJ, Staforelli JP, Villena F and Strzalka K, 2015: *An in vitro study on the antioxidant capacity of usnic acid on human erythrocytes and molecular models of its membrane.* Biochim Biophys Acta. 1848:2829-38.

Thiry M and Lafontaine DL, 2005: *Birth of a nucleolus: the evolution of nucleolar compartments.* Trends Cell Biol. 15:194-9.

Warner JR, 1999: *The economics of ribosome biosynthesis in yeast.* Trends Biochem Sci. 24:437-40

Woolford JL and Baserga SJ, 2013: *Ribosome biogenesis in the yeast Saccharomyces cerevisiae.* Genetics. 195:643-81.

Yokouchi Y, Imaoka M, Niino N, Kiyosawa N, Sayama A and Jindo T, 2015: *(+)-Usnic acid-induced myocardial toxicity in rats.* Toxicol Pathol. 43:424-34.